Radiation in the Atmosphere

A Course in Theoretical Meteorology

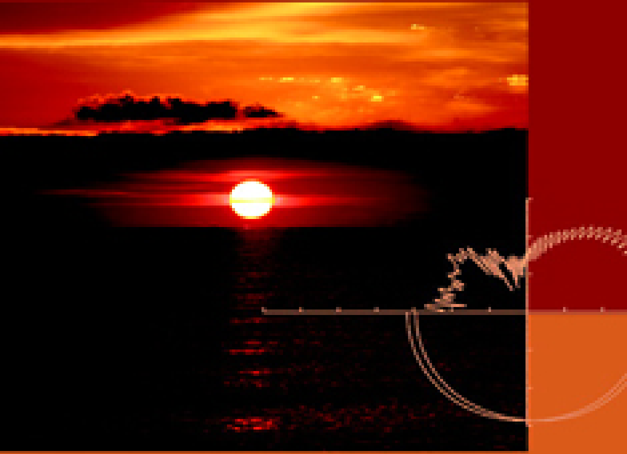

Wilford Zdunkowski, Thomas Trautmann, and Andreas Bott

CAMBRIDGE

CAMBRIDGE www.cambridge.org/9780521871075

This page intentionally left blank

RADIATION IN THE ATMOSPHERE
A Course in Theoretical Meteorology

This book presents the theory and applications of radiative transfer in the atmosphere. It is written for graduate students and researchers in the fields of meteorology and related sciences.

The book begins with important basic definitions of the radiative transfer theory. It presents the hydrodynamic derivation of the radiative transfer equation and the principles of invariance. The authors examine in detail various quasi-exact solutions of the radiative transfer equation, such as the matrix operator method, the discrete ordinate method, and the Monte Carlo method. A thorough treatment of the radiative perturbation theory is given. The book also presents various two-stream methods for the approximate solution of the radiative transfer equation. The interaction of radiation with matter is discussed as well as the transmission in individual spectral lines and in bands of lines. It formulates the theory of gaseous absorption and analyzes the normal vibrations of linear and non-linear molecules. The book presents the Schrödinger equation and describes the computation of transition probabilities, before examining the mathematical formulation of spectral line intensities. A rigorous treatment of Mie scattering is given, including Rayleigh scattering as a special case, and the important efficiency factors for extinction, scattering and absorption are derived. Polarization effects are introduced with the help of Stokes parameters. The fundamentals of remote sensing applications of radiative transfer are presented.

Problems of varying degrees of difficulty are included at the end of each chapter, so readers can further their understanding of the materials covered in the book.

WILFORD ZDUNKOWSKI is Professor Emeritus at the Institute of Atmospheric Physics in the University of Mainz, Germany.

THOMAS TRAUTMANN is Head of the Unit for Atmospheric Processors at the Remote Sensing Technology Institute, German Aerospace Center (DLR) Oberpfaffenhofen, Germany, and Professor for Meteorology at the University of Leipzig, Germany.

ANDREAS BOTT is a university professor for Theoretical Meteorology at the Meteorological Institute of the University of Bonn, Germany.

Together, the authors have a wealth of experience in teaching atmospheric physics, including courses on atmospheric thermodynamics, atmospheric dynamics, cloud microphysics, atmospheric chemistry, and numerical modeling. Professors Zdunkowski and Bott co-wrote *Dynamics of the Atmosphere* and *Thermodynamics of the Atmosphere* (Cambridge University Press 2003 and 2004).

RADIATION IN THE ATMOSPHERE

A Course in Theoretical Meteorology

WILFORD ZDUNKOWSKI
Formerly University of Mainz, Germany

THOMAS TRAUTMANN
German Aerospace Center (DLR), Germany

ANDREAS BOTT
University of Bonn, Germany

CAMBRIDGE
UNIVERSITY PRESS

CAMBRIDGE UNIVERSITY PRESS
Cambridge, New York, Melbourne, Madrid, Cape Town, Singapore, São Paulo

Cambridge University Press
The Edinburgh Building, Cambridge CB2 8RU, UK

Published in the United States of America by Cambridge University Press, New York

www.cambridge.org
Information on this title: www.cambridge.org/9780521871075

First published in print format 2007

ISBN-13 978-0-511-27175-5 eBook (Adobe Reader)
ISBN-10 0-511-27175-1 eBook (Adobe Reader)

ISBN-13 978-0-521-87107-5 hardback
ISBN-10 0-521-87107-7 hardback

This book is dedicated to the memory of
Professor Fritz Möller (1906–1983) and
Professor J. Vern Hales (1917–1997).
We have profited directly and indirectly
from their lectures and research.

Contents

Preface

Radiation in the Atmosphere is the third volume in the series *A Course in Theoretical Meteorology*. The first two volumes entitled *Dynamics of the Atmosphere* and *Thermodynamics of the Atmosphere* were first published in the years 2003 and 2004.

The present textbook is written for graduate students and researchers in the field of meteorology and related sciences. Radiative transfer theory has reached a high point of development and is still a vastly expanding subject. Kourganoff (1952) in the postscript of his well-known book on radiative transfer speaks of the three olympians named completeness, up-to-date-ness and clarity. We have not made any attempt to be complete, but we have tried to be reasonably up-to-date, if this is possible at all with the many articles on radiative transfer appearing in various monthly journals. Moreover, we have tried very hard to present a coherent and consistent development of radiative transfer theory as it applies to the atmosphere. We have given principle allegiance to the olympian clarity and sincerely hope that we have succeeded.

In the selection of topics we have resisted temptation to include various additional themes which traditionally belong to the fields of physical meteorology and physical climatology. Had we included these topics, our book, indeed, would be very bulky, and furthermore, we would not have been able to cover these subjects in the required depth. Neither have we made any attempt to include radiative transfer theory as it pertains to the ocean, a subject well treated by Thomas and Stamnes (1999) in their book *Radiative Transfer in the Atmosphere and Ocean*.

As in the previous books of the series, we were guided by the principle to make the book as self-contained as possible. As far as space would permit, all but the most trivial mathematical steps have been included in the presentation of the theory to encourage students to follow the various developments. Nevertheless, here and there students may find it difficult to follow our reasoning. In this case, we encourage them not to get stuck with a particular detail but to continue with the subject. Additional details given later may clarify any questions. Moreover, on a second reading everything will become much clearer.

We will now give a brief description of the various chapters and topics treated in this book. Chapter 1 gives the general introduction to the book. Various important definitions such as the radiance and the net flux density are given to describe the radiation field. The interaction of radiation with matter is briefly discussed by introducing the concepts of absorption and scattering. To get an overall view of the mean global radiation budget of the system Earth–atmosphere, it is shown that the incoming and outgoing energy at the top of the atmosphere are balanced.

In Chapter 2 the hydrodynamic derivation of the radiative transfer equation (RTE) is worked out; this is in fact the budget equation for photons. The radiatively induced temperature change is formulated with the help of the first law of thermodynamics. Some basic formulas from spherical harmonics, which are needed to evaluate certain transfer integrals, are presented. Various special cases are discussed.

Chapter 3 presents the principle of invariance which, loosely speaking, is a collection of common sense statements about the exact mathematical structure of the radiation field. At first glance the mathematical formalism looks much worse than it really is. A systematic study of the mathematical and physical principles of invariance it quite rewarding.

Quasi-exact solutions of the RTE, such as the matrix operator method together with the doubling algorithm are presented in Chapter 4. Various other prominent solutions such as the successive order of scattering and the Monte Carlo methods are discussed in some detail.

Chapter 5 presents the radiative perturbation theory. The concept of the adjoint formulation of the RTE is introduced, and it is shown that in the adjoint formulation certain radiative effects can be evaluated with much higher numerical efficiency than with the so-called forward mode methods.

For many practical purposes in connection with numerical weather prediction it is sufficient to obtain fast approximate solutions of the RTE. These are known as two-stream methods and are treated in Chapter 6. Partial cloudiness is introduced in the solution scheme on the basis of two differing assumptions. The method allows fairly general situations to be handled.

In Chapter 7, the theory of individual spectral lines and band models is treated in some detail. In those cases in which scattering effects can be ignored, formulas are worked out to describe the mean absorption of homogeneous atmospheric layers. A technique is introduced which makes it possible to replace the transmission through an inhomogeneous atmosphere by a nearly equivalent homogeneous layer.

The theory of gaseous absorption is formulated in Chapter 8. The analysis of normal vibrations of linear and nonlinear molecules is introduced. The Schrödinger equation is presented and the computation of transition probabilities is described, which finally leads to the mathematical formulation of spectral line intensities. Simple but instructive analytic solutions of Schrödinger's equation are obtained leading, for example, to the description of the vibration–rotation spectrum of diatomic molecules.

Not only atmospheric gaseous absorbers influence the radiation field but also aerosol particles and cloud droplets. Chapter 9 gives a rigorous treatment of Mie scattering which includes Rayleigh scattering as a special case. The important efficiency factors for extinction, scattering and absorption are derived. The mathematical analysis requires the mathematical skill which the graduate student has acquired in various mathematics and physics courses. The effects of nonspherical particles are not treated in this book.

So far polarization has not been included in the RTE, which is usually satisfactory for energy considerations but may not be sufficient for optical applications. To give a complete description of the radiation field the polarization effects are introduced in Chapter 10 with the help of the Stokes parameters. This finally leads to the most general vector formulation of the RTE in terms of the phase matrix while the phase function is sufficient if polarization may be ignored.

Chapter 11 introduces remote sensing applications of radiative transfer. After the general description of some basic ideas, the RTE is presented in a form which is suitable to recover the atmospheric temperature profile by special inversion techniques. The chapter closes with a description of the way in which the atmospheric ozone profile can be retrieved using radiative perturbation theory.

The book closes with Chapter 12 in which a simple and brief account of the influence of clouds on climate is given. The student will be exposed to concepts such as cloud forcing and cloud radiative feedback.

Problems of various degrees of difficulty are included at the end of each chapter. Some of the included problems are almost trivial. They serve the purpose of making students familiar with new concepts and terminologies. Other problems are more demanding. Where necessary answers to problems are given at the end of the book.

One of the problems that any author of a physical science textbook is confronted with, is the selection of proper symbols. Inspection of the book shows that many times the same symbol is used to label several quite different physical entities. It would be ideal to represent each physical quantity by a unique symbol which is not used again in some other context. Consider, for example, the letter k. For the Boltzmann constant we could have written k_{B}, for Hooke's constant k_{H}, for the wave number k_{w}, and k_{s} for the climate sensitivity constant. It would have been possible, in addition to using the Greek alphabet, to also employ the letters of another alphabet, e.g. Hebrew, to label physical quantities in order to obtain uniqueness in notation. Since usually confusion is unlikely, we have tried to use standard notation even if the same symbol is used more than once. For example, the climate sensitivity parameter k appears in Chapter 12, Hooke's constant in Chapter 8 and Boltzmann's constant in Chapter 1.

The book concludes with a list of frequently used symbols and a list of constants.

We would like to give recognition to the excellent textbooks *Radiative Transfer* by the late S. Chandrasekhar (1960), to *Atmospheric Radiation* by R. M. Goody (1964) and the updated version of this book by Goody and Yung (1989). These books have been an invaluable guidance to us in research and teaching.

We would like to give special recognition to Dr W. G. Panhans for his splendid cooperation in organizing and conducting our exercise classes. Recognition is due to Dr Jochen Landgraf for discussions related to the perturbation theory and to ozone retrieval. Moreover, we will be indebted to Sebastian Otto for carrying out the transfer calculations presented in Section 7.5. We also wish to express our gratitude to many colleagues and graduate students for helpful comments while preparing the text. Last but not least we wish to thank our families for their patience and encouragement during the preparation of this book.

It seems to be one of the unfortunate facts of life that no book as technical as this one can be written free of error. However, each author takes comfort in the thought that any errors appearing in this book are due to one of the other two. To remove such errors, we will be grateful for anyone pointing these out to us.

1

Introduction

1.1 The atmospheric radiation field

The theory presented in this book applies to the lower 50 km of the Earth's atmosphere, that is to the troposphere and to the stratosphere. In this part of the atmosphere the so-called *local thermodynamic equilibrium* is observed.

In general, the condition of *thermodynamic equilibrium* is described by the state of matter and radiation inside a constant temperature enclosure. The radiation inside the enclosure is known as *black body radiation*. The conditions describing thermodynamic equilibrium were first formulated by Kirchhoff (1882). He stated that within the enclosure the radiation field is:

(1) isotropic and unpolarized;
(2) independent of the nature and shape of the cavity walls;
(3) dependent only on the temperature.

The existence of local thermodynamic equilibrium in the atmosphere implies that a local temperature can be assigned everywhere. In this case the *thermal radiation* emitted by each atmospheric layer can be described by *Planck's radiation law*. This results in a relatively simple treatment of the thermal radiation transport in the lower sections of the atmosphere.

Kirchhoff's and Planck's laws, fundamental in radiative transfer theory, will be described in the following chapters. While the derivation of Planck's law requires a detailed microscopic picture, Kirchhoff's law may be obtained by using purely thermodynamic arguments. The derivation of Kirchhoff's law is presented in numerous textbooks such as in *Thermodynamics of the Atmosphere* by Zdunkowski and Bott (2004).[1]

[1] Whenever we make reference to this book, henceforth we simply refer to THD (2004).

The atmosphere, some sort of an open system, is not in thermodynamic equilibrium since the temperature and the radiation field vary in space and in time. Nevertheless, in the troposphere and within the stratosphere the *emission* of thermal radiation is still governed by Kirchhoff's law at the local temperature. The reason for this is that in these atmospheric regions the density of the air is sufficiently high so that the mean time between molecular collisions is much smaller than the mean lifetime of an excited state of a radiating molecule. Hence, equilibrium conditions exist between *vibrational* and *rotational* and the *translational energy* of the molecule. At levels higher than 50 km, the two time scales become comparable resulting in a sufficiently strong deviation from thermodynamic equilibrium so that Kirchhoff's law cannot be applied anymore.

The breakdown of thermodynamic equilibrium in higher regions of the atmosphere also implies that Planck's law no longer adequately describes the *thermal emission* so that quantum theoretical arguments must be introduced to describe radiative transfer. Quantum theoretical considerations of this type will not be treated in this book. For a study of this situation we refer the reader to the textbook *Atmospheric Radiation* by Goody and Yung (1989).

The units usually employed to measure the wavelength of radiation are the micrometer (μm) with $1\,\mu\text{m} = 10^{-6}$ m or the nanometer (nm) with $1\text{ nm} = 10^{-9}$ m and occasionally Ångströms (Å) where $1\text{ Å} = 10^{-10}$ m. The thermal radiation spectrum of the Sun, also called the *solar radiation spectrum*, stretches from roughly 0.2–3.5 μm where practically all the thermal energy of the solar radiation is located. It consists of ultraviolet radiation (< 0.4 μm), visible radiation (0.4–0.76 μm), and infrared radiation > 0.76 μm. The thermal radiation spectrum of the Earth ranges from about 3.5–100 μm so that for all practical purposes the solar and the terrestrial radiation spectrum are separated. As will be seen later, this feature is of great importance facilitating the calculation of atmospheric radiative transfer. Due to the positions of the spectral regions of the solar and the terrestrial radiation we speak of *short-wave* and *long-wave radiation*. The terrestrial radiation spectrum is also called the *infrared radiation spectrum*.

Important applications of atmospheric radiative transfer are climate modeling and weather prediction which require the evaluation of a prognostic temperature equation. One important term in this equation, see e.g. Chapter 3 of THD (2004), is the divergence of the *net radiative flux density* whose evaluation is fairly involved, even for conditions of local thermodynamic equilibrium. Accurate numerical radiative transfer algorithms exist that can be used to evaluate the radiation part of the temperature prediction equation. In order to judiciously apply any such computer model, some detailed knowledge of radiative transfer is required.

There are other areas of application of radiative transfer such as remote sensing. In the concluding chapter of this textbook we will present various examples.

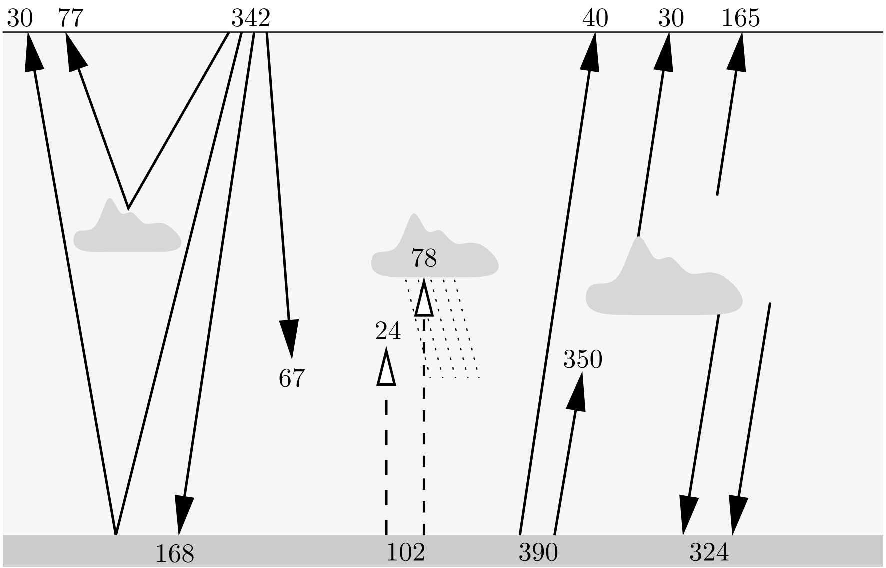

Fig. 1.1 The Earth's annual global mean energy budget, after Kiehl and Trenberth (1997), see also Houghton *et al.* (1996). Units are (W m^{-2}).

1.2 The mean global radiation budget of the Earth

Owing to the advanced satellite observational techniques now at our disposal, we are able to study with some confidence the Earth's annual mean global energy budget. Early meteorologists and climatologists have already understood the importance of this topic, but they did not have the observational basis to verify their results. A summary of pre-satellite investigations is given by Hunt *et al.* (1986). In the following we wish to briefly summarize the mean global radiation budget of the Earth according to Kiehl and Trenberth (1997). Here we have an instructive example showing in which way radiative transfer models can be applied to interpret observations.

The evaluation of the radiation model requires vertical distributions of absorbing gases, clouds, temperature, and pressure. For the major absorbing gases, namely water vapor and ozone, numerous observational data must be handled and supplemented with model atmospheres. In order to calculate the important influence of CO_2 on the infrared radiation budget, Kiehl and Trenberth specify a constant volume mixing ratio of about 350 ppmv. Moreover, it is necessary to employ distributions of the less important absorbing gases CH_4, N_2O, and of other trace gases. Using the best data presently available, they have provided the radiation budget as displayed in Figure 1.1.

The analysis employs a *solar constant* $S_0 = 1368\,\mathrm{W\,m^{-2}}$. This is the solar radiation, integrated over the entire solar spectral region which is received by the Earth per unit surface perpendicular to the solar beam at the mean distance between the Earth and the Sun. Since the circular cross-section of the Earth is exposed to the parallel solar rays, each second our planet receives the energy amount $\pi R^2 S_0$ where R is the radius of the Earth. On the other hand, the Earth emits infrared radiation from its entire surface $4\pi R^2$ which is four times as large as the cross-section. Thus for energy budget considerations we must distribute the intercepted solar energy over the entire surface so that, on the average, the Earth's surface receives $1/4$ of the solar constant. This amounts to a solar input of $342\,\mathrm{W\,m^{-2}}$ as shown in the figure.

The measured solar radiation reflected to space from the Earth's surface–atmosphere system amounts to about $107\,\mathrm{W\,m^{-2}}$. The ratio of the reflected to the incoming solar radiation is known as the *global albedo* which is close to 31%. Early pre-satellite estimates of the global albedo resulted in values ranging from 40–50%. With the help of radiation models and measurements it is found that cloud reflection and scattering by atmospheric molecules and aerosol particles contribute $77\,\mathrm{W\,m^{-2}}$ while ground reflection contributes $30\,\mathrm{W\,m^{-2}}$. In order to have a balanced radiation budget at the top of the atmosphere, the net gain $342 - 107 = 235\,\mathrm{W\,m^{-2}}$ of the short-wave solar radiation must be balanced by emission of long-wave radiation to space. Indeed, this is verified by satellite measurements of the outgoing long-wave radiation.

Let us now briefly consider the radiation budget at the surface of the Earth, which can be determined only with the help of radiation models since sufficiently dense surface measurements are not available. Assuming that the ground emits black body radiation at the temperature of $15\,^\circ\mathrm{C}$, an amount of $390\,\mathrm{W\,m^{-2}}$ is lost by the ground. According to Figure 1.1 this energy loss is partly compensated by a short-wave gain of $168\,\mathrm{W\,m^{-2}}$ and by a long-wave gain of $324\,\mathrm{W\,m^{-2}}$ because of the thermal emission of the atmospheric *greenhouse gases* (H_2O, CO_2, O_3, CH_4, etc.) and clouds. Thus the total energy gain $168 + 324 = 492\,\mathrm{W\,m^{-2}}$ exceeds the long-wave loss of $390\,\mathrm{W\,m^{-2}}$ by $102\,\mathrm{W\,m^{-2}}$.

In order to have a balanced energy budget at the Earth's surface, other physical processes must be active since a continuous energy gain would result in an ever increasing temperature of the Earth's surface. From observations, Kiehl and Trenberth estimated a mean global precipitation rate of $2.69\,\mathrm{mm\,day^{-1}}$ enabling them to compute a surface energy loss due to evapotranspiration. Multiplying $2.69\,\mathrm{mm\,day^{-1}}$ by the density of water and by the latent heat of vaporization amounts to a latent heat flux density of $78\,\mathrm{W\,m^{-2}}$. Thus the surface budget is still unbalanced by $24\,\mathrm{W\,m^{-2}}$. Assigning a surface energy loss of $-24\,\mathrm{W\,m^{-2}}$ resulting from sensible heat fluxes yields a balanced energy budget at the Earth's surface. The individual losses due to turbulent surface fluxes are uncertain within several percent since it is very difficult to accurately assess the global amount of precipitation which implies that the estimated sensible heat flux density is also quite uncertain. Only the sum of the turbulent surface flux densities is reasonably certain.

Finally, we must study the budget of the atmosphere itself. Figure 1.1 reveals that the atmosphere gains 67 W m^{-2} by absorption of solar radiation, 102 W m^{-2} by turbulent surface fluxes, and additionally 350 W m^{-2} resulting from long-wave radiation emitted by the surface of the Earth and intercepted by atmospheric greenhouse gases and clouds. The total of 519 W m^{-2} must be re-emitted by the atmosphere. As shown in the figure, the atmospheric greenhouse gases and the clouds emit $165 + 30 = 195$ W m^{-2} to space and 324 W m^{-2} as back-radiation to the surface of the Earth just balancing the atmospheric energy gain.

We also see that from the 390 W m^{-2} emitted by the Earth's surface only 350 W m^{-2} are intercepted by the atmosphere. To account for the remaining 40 W m^{-2} we recognize that these escape more or less unimpeded to space in the so-called *spectral window region* as will be discussed later.

By considering the budget in Figure 1.1, we observe that only the reflected solar radiation and the long-wave radiation emitted to space are actually verified by measurements. However, the remaining budget components should also be taken seriously since nowadays radiation models are quite accurate. Nevertheless, the output of the models cannot be any more accurate than the input data. In future days further refinements and improvements of the global energy budget can be expected.

In order to calculate the global radiation budget, we must have some detailed information on the absorption behavior of atmospheric trace gases and the physical properties of aerosol and cloud particles. In a later chapter we will study the radiative characteristics of spherical particles by means of the solution of *Maxwell's equations* of electromagnetic theory. Here we will only qualitatively present the absorption spectrum of the most important greenhouse gases.

Figure 1.2 combines some important information regarding the solar spectrum. The upper curve labeled TOA (top of the atmosphere) shows the extraterrestrial incoming solar radiation after Coulson (1975). For wavelengths exceeding 1.4 μm this curve coincides closely with a Planckian black body curve of 6000 K. The lower curve depicts the total solar radiation reaching the Earth's surface for a solar zenith angle $\theta_0 = 60°$. The calculations were carried out with sufficiently high spectral resolution using the so-called Moderate Resolution Atmospheric Radiance and Transmittance Model (MODTRAN; version 3.5; Anderson, 1996; Kneizys *et al.*, 1996) program package. All relevant absorbing trace gases shown in the figure are included in the calculations. Not shown are the positions of the CO and CH_4 absorption bands which are located in the solar spectrum and in the near infared spectral region of

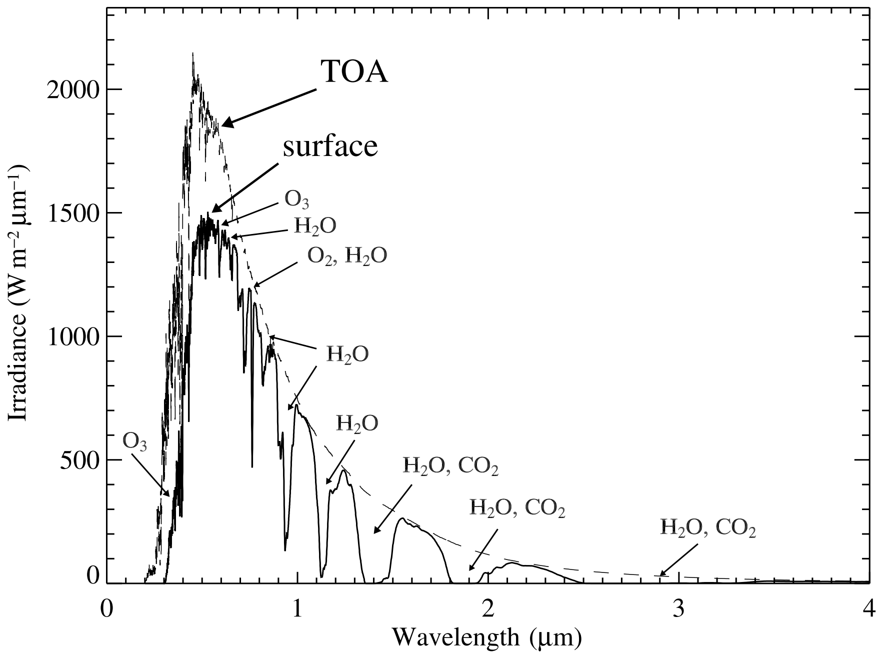

Fig. 1.2 Incoming solar flux density at the top of the atmosphere (TOA) and at ground level. The solar zenith angle is $\theta_0 = 60°$, ground albedo $A_g = 0$. The spectral positions of major absorption bands of the trace gases are shown.

thermal radiation. A tabulation of bands of these two trace gases is given, for example, in Goody (1964a). Since the radiation curve for ground level shows a high spectral variability, it was artificially smoothed for better display to a somewhat lower spectral resolution.

Figure 1.3 depicts the spectral distribution of the upwelling thermal radiance as a function of the wave number (to be defined later) at a height of 60 km. For comparison purposes the Planck black body radiance curves for several temperatures are shown also. The maximum of the 300 K black body curve is located at roughly 600 cm^{-1}. The calculations were carried out with the same program package (MODTRAN) using a spectral resolution of 1 cm^{-1}. All relevant absorbing and emitting gases have been accounted for. The widths of the major infrared absorption bands (H_2O, CO_2, O_3) are also shown in the figure.

Kiehl and Trenberth (1997) produced similar curves for the solar and infrared radiative fluxes per unit surface. However, in addition to the absorption by gases shown in Figures 1.2 and 1.3, they also included the effects of clouds in their calculations by assuming an effective droplet radius of 10 µm and suitable liquid water contents. Moreover, assumptions were made about the spatial distributions of clouds. Their results indicate that water vapor is the most important

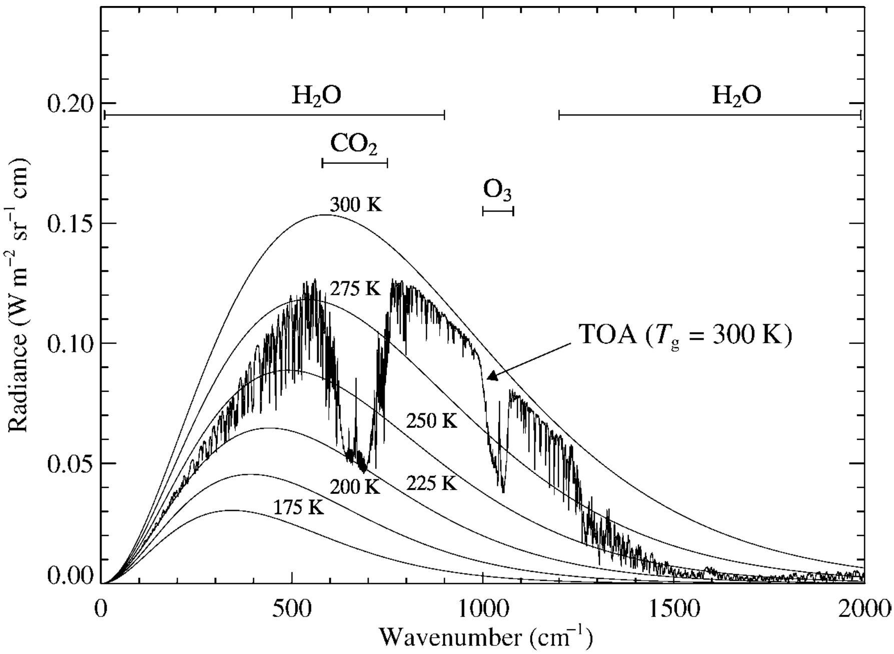

Fig. 1.3 Upwelling infrared radiance at a height of 60 km for a clear sky mid-latitude summer atmosphere.

gas absorbing 38 W m^{-2} of solar radiation which is followed by O_3 (15 W m^{-2}) and O_2 (2 W m^{-2}) while the effect of CO_2 may be ignored. Thus the greenhouse gases absorb 55 W m^{-2}. Figure 1.1, however, requires 67 W m^{-2}. The 12 W m^{-2} still missing must be attributed to partial cloudiness and to spectral overlap effects, i.e., cloud droplets and gases absorb at the same wavelength. Handling clouds in the radiative transfer problem is usually very difficult since in general water droplet size distributions are unknown.

Finally, let us consider the gaseous absorption bands of the infrared spectrum. In the calculations of Kiehl and Trenberth (1997) analogous to Figure 1.3, the surface is assumed to emit black body radiation with a temperature of 15°C. The major absorbing gases are H_2O, O_3, and CO_2. Of course, the same distribution of absorbing gases and clouds as for solar radiation is assumed. Integration of the infrared curve at the top of the atmosphere over the entire spectral region yields 235 W m^{-2} as required by Figure 1.1.

We conclude this section by considering a simple example to obtain the effective emission temperature of the system Earth's surface–atmosphere. As we have discussed above, the cross-section of the Earth intercepts the solar energy $\pi R^2 S_0$. Since the global albedo is 31%, the rate of absorption is $1368(1-0.31) = 944$ W m^{-2}. Assuming that the Earth emits black body radiation, we must apply the

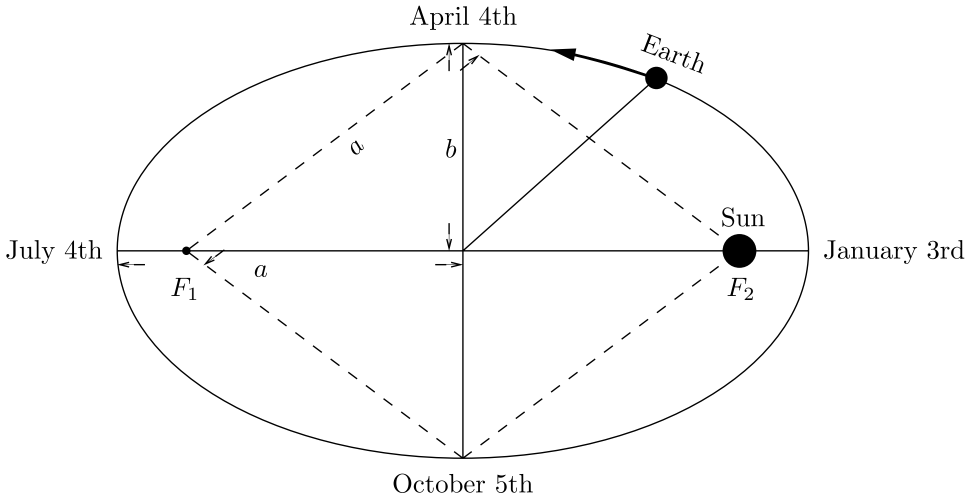

Fig. 1.4 Simplified elliptical geometry of the Earth's orbit.

well-known *Stefan–Boltzmann law* so that the Earth's surface emits $4\pi R^2\sigma T^4$ where σ is the *Stefan–Boltzmann constant*. Assuming steady-state conditions, we have $\pi R^2 \times 944$ W m$^{-2} = 4\pi R^2\sigma T^4$ from which we obtain the temperature $T = 254$ K which resembles the effective emission temperature of our planet.

1.3 Solar–terrestrial relations

To a high degree of accuracy the Earth's orbit around the Sun can be described by an ellipse with eccentricity $e = \sqrt{a^2 - b^2}/a = 0.01673$, where a and b are, respectively, the semi-major and semi-minor axis of the ellipse, see Figure 1.4. The Sun's position is located in one of the two elliptical foci (F_1, F_2). For demonstration purposes, the figure exaggerates the eccentricity of the elliptical orbit. The *perihelion*, that is the shortest distance $r_{\min}$ between Sun and Earth, occurs around January 3rd, while the *aphelion*, that is the largest distance $r_{\max}$ between Sun and Earth, is registered around July 4th. These times are not constant, but they vary from year to year. Often the mean distance between the Earth and the Sun is approximated by

$$a = \frac{r_{\min} + r_{\max}}{2} = 1.496 \times 10^8 \,\text{km} \tag{1.1}$$

The distances $r_{\min}$ and $r_{\max}$ are related to a and e via

$$\begin{aligned} r_{\min} &= a(1 - e) = 1.471 \times 10^8 \,\text{km} \\ r_{\max} &= a(1 + e) = 1.521 \times 10^8 \,\text{km} \end{aligned} \tag{1.2}$$

Beginning with January 1st, i.e. Julian day number 1 of the year, a normal year counts 365 days (for simplicity we will not take the occurrence of leap years into account). A particular day of the year is then labelled with its corresponding Julian day number J.

We introduce the rotation angle Γ of the Earth beginning with the 1st of January as

$$\Gamma = \frac{2\pi}{365}(J - 1) \tag{1.3}$$

where Γ is expressed in radians.

During the course of the year the angular distance Sun–Earth, the *solar declination* δ, and the so-called *equation of time* ET change in a more or less harmonic manner. In the following we will discuss simple expressions developed by Spencer (1971) which are accurate enough to evaluate the quantities $(a/r)^2$, δ, and ET, where r is the actual distance between Sun and Earth. The term $(a/r)^2$ is given by

$$\begin{aligned}\left(\frac{a}{r}\right)^2 &= 1.000110 + 0.034221\cos\Gamma + 0.001280\sin\Gamma \\ &\quad + 0.000719\cos 2\Gamma + 0.000077\sin 2\Gamma\end{aligned} \tag{1.4}$$

with a maximum error of approximately 10^{-4}. If $S_0 = 1368\,\mathrm{W\,m^{-2}}$ is the *solar constant* for the mean distance between Sun and Earth, the actual solar constant varies as a function of J

$$S_0(J) = S_0\left(\frac{a}{r(J)}\right)^2 \tag{1.5}$$

According to (1.4) the maximum change of $S_0(J)$ relative to S_0 has an amplitude of approximately 3.3%.

The solar declination δ is defined as the angle between the Earth's equatorial plane and the actual position of the Sun as seen from the center of the Earth. The Earth's rotational axis and the normal to the Earth's plane of the ecliptic make on average an angle of $\varepsilon = 23°27'$, δ amounts to $+23°27'$ and $-23°27'$ at summer solstice (around June 21st) and winter solstice (around December 22nd), respectively. These relations are illustrated in Figure 1.5 and in the three-dimensional view of the Sun–Earth geometry of Figure 1.6.

The *equinox points* are defined as the intersecting line (equinox line) between the Earth's plane of the ecliptic and the Sun's equatorial plane. A second line which is normal to the equinox line and which is located in the Earth's plane of the ecliptic intersects the Earth's orbit in the points WS (winter solstice) and SS (summer solstice). The perihelion P and the aphelion A, which both lie on the semi-major axis of the Earth's elliptical orbit, make an angle $\psi = 11°08'$ with the solstice line.

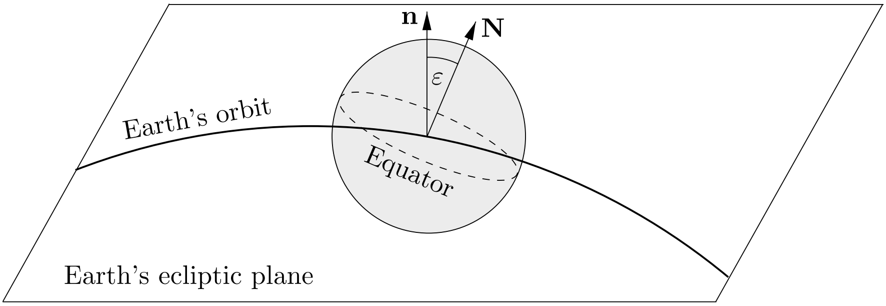

Fig. 1.5 Relation between the Earth's orbit, the normal vector **n** to the plane of the ecliptic, the Earth's rotational vector **N** and the angle of the ecliptic ε.

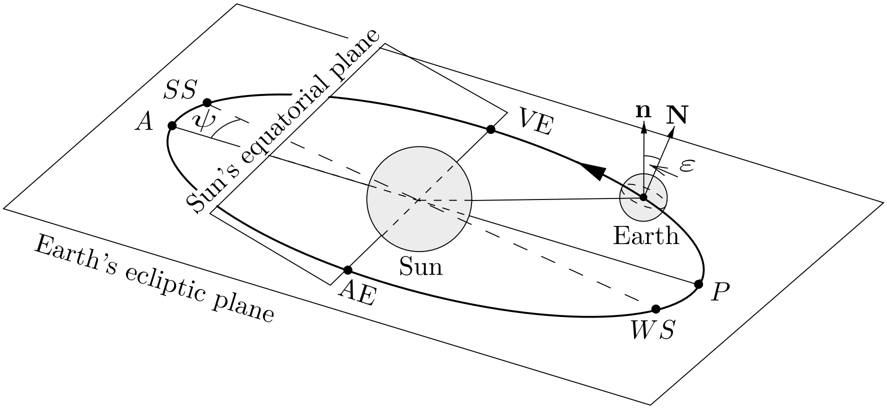

Fig. 1.6 Schematical view of the Sun–Earth geometry. P, perihelion; VE, vernal equinox; SS, summer solstice; A, aphelion; AE, autumnal equinox; WS, winter solstice; ε, angle of the ecliptic; ψ, angle between the distances (SS, WS) and (A, P); **N**, vector along the rotational axis of the Earth; **n**, normal unit vector with respect to the Earth's plane of the ecliptic.

It should be observed that the vector **N** is fixed in direction pointing to the polar star. At the solstices the vectors **N**, **n** and the line between the solstice points lie in the same plane so that $\delta = \pm\, 23^{\circ}27'$. At the equinox points ($\delta = 0^{\circ}$) the line between the Earth and the Sun is at a right angle to the line (SS, WS).

The solar declination δ is a function of the Julian day number J. It can be expressed as

$$\begin{aligned}\delta = {} & 0.006918 - 0.399912\cos\Gamma + 0.070257\sin\Gamma \\ & - 0.006758\cos 2\Gamma + 0.000907\sin 2\Gamma \qquad (1.6)\end{aligned}$$

with δ expressed in radians. Due to Spencer (1971) this approximate formula has an error in δ less than $12'$. Figure 1.7 depicts a plot of δ versus J.

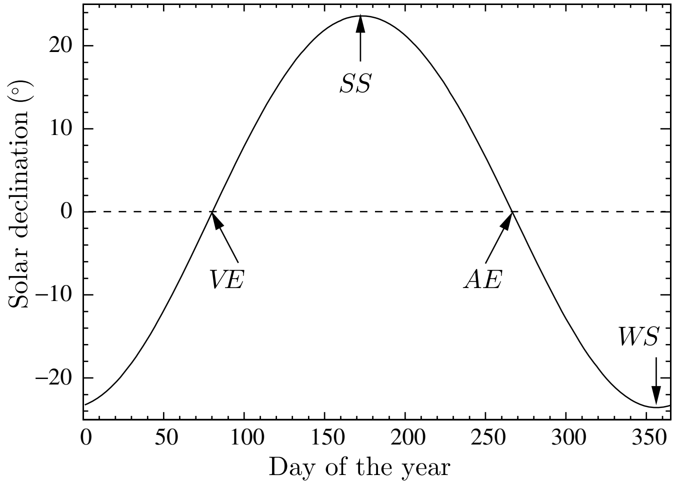

Fig. 1.7 Variation of the solar declination δ as a function of the Julian day J, see (1.6). VE, vernal equinox; SS, summer solstice; AE, autumnal equinox; WS, winter solstice.

1.3.1 The equation of time

In the following we assume that the period of the rotation of the Earth around the North Pole is constant. The time interval between two successive passages of a fixed star as seen from the local meridian of an observer on the Earth's surface is called a *sidereal day*. Due to the fact that the Earth moves around the Sun in an elliptical orbit, the time interval between two successive passages of the Sun in the local meridian, i.e. the so-called *solar day*, is about 4 min longer than the length of the sidereal day.

For a practical definition of time, one introduces the so-called *mean solar day* which is exactly divided into 24-h periods. Thus the local noon with respect to the local mean time (LMT) is defined by the passage of a mean fictitious Sun as registered from the Earth observer's local meridian. Clearly, depending on the Julian day J the real Sun appears somewhat earlier or later in the local meridian than the fictitious Sun. The time difference between the noon of the *true solar time* (TST) and the noon of the *local mean time* (LMT) is the so-called *equation of time* ET

$$\boxed{ET = TST - LMT} \tag{1.7}$$

Following the analysis of Spencer (1971), a functional fit expression can be derived for ET in the form

$$\begin{aligned} ET = \frac{1440}{2\pi}(&0.000075 + 0.001868\cos\Gamma - 0.032077\sin\Gamma \\ &- 0.014615\cos 2\Gamma - 0.040849\sin 2\Gamma) \end{aligned} \tag{1.8}$$

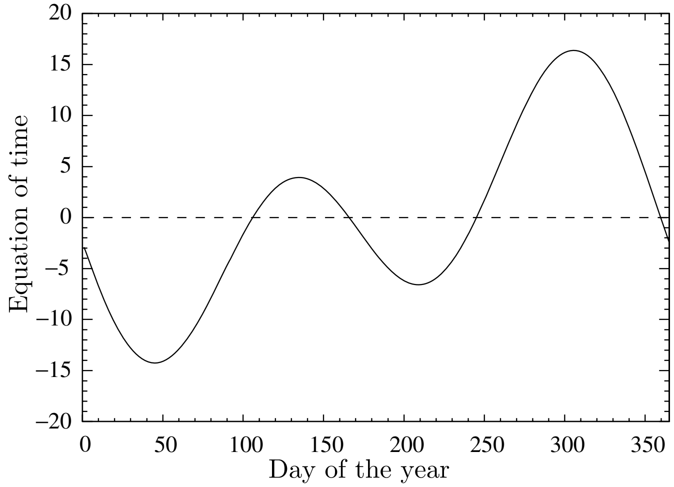

Fig. 1.8 Variation of the equation of time ET (in minutes) during the course of the year as given by (1.8).

where ET is expressed in minutes and 1440 is the number of minutes per day. The accuracy of this approximation is better than 35 s. The maximum time difference between TST and LMT amounts to less than about ± 15 min. Figure 1.8 depicts the variation of ET during the course of the year. Note that the irregularities of the Earth's orbit around the Sun lead to a complicated shape of the functional form of ET versus J.

Universal time UT, or *Greenwich mean time GMT*, is defined as the LMT at Greenwich's (UK) meridian at 0° in longitude. Since 24 h cover an entire rotation of the Earth, LMT increases by exactly 1 h per 15° in eastern longitude, i.e. 4 min per degree of eastern longitude. Similarly, LMT decreases by 4 min if one moves by one degree of longitude in the western direction. For the true solar time we thus obtain the relation

$$\boxed{TST = UT + 4\lambda + ET} \tag{1.9}$$

where TST, UT, and ET are given in minutes and the longitude λ is in units of degree ($-180^\circ < \lambda \leq 180^\circ$).

The *hour angle of the Sun H* is defined as the angle between the local observer's meridian and the solar meridian, see Figure 1.9. If H is expressed in degrees longitude one obtains

$$H = 15(12 - TST) \tag{1.10}$$

where TST has to be inserted in hours. Note that $H > 0$ in the morning and $H < 0$ in the afternoon.

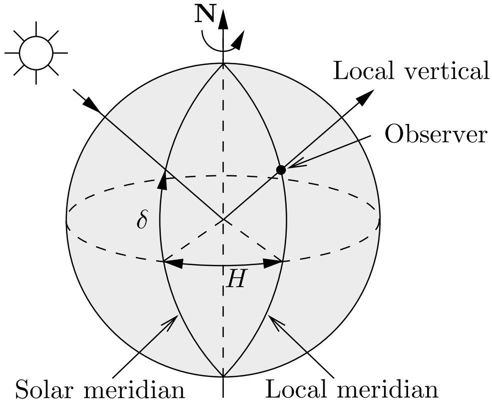

Fig. 1.9 Relation between hour angle H, solar declination δ, the solar and the local meridian.

The *local standard time* LST is defined as the local mean time for a given meridian being a multiple of 15° away from the Greenwich meridian (0°). Therefore, LST and UT differ by an integral number of hours. For particular countries, differences of 30 and 45 min relative to the standard time meridians have been introduced for convenience. Note also that for locations with daylight saving time, the local mean time differs by 1 to 2 h relative to LST.

1.3.2 Geographical coordinates and the solar position

A particular point P on the Earth's surface is identified by the pair of *geographical coordinates* (λ, ϕ), where λ is the longitude and ϕ is the latitude. Note that ϕ is counted positive in the northern hemisphere and negative in the southern hemisphere. The coordinates of the Sun relative to P are defined by the *solar zenith angle* ϑ_0 and the solar *azimuth angle* φ_0. If the Sun is at the zenith we have $\vartheta_0 = 180°$, and $\vartheta_0 = 90°$ if it is at the horizon, see Figure 1.10. The *solar height* h is given by $h = \vartheta_0 - \pi/2$. The solar azimuth φ_0 is defined as the angle between the solar vertical plane and a vertical plane of reference which is aligned with the north–south direction. Here, $\varphi_0 = 0°$ if the Sun is exactly over the southern direction and φ_0 is counted positive in the eastward direction. Figure 1.11 depicts the apparent track of the Sun during the day.

The position angles (ϑ_0, φ_0) of the Sun are usually not measured directly and must be determined from other known angles. Utilizing the laws of spherical trigonometry it can be shown that the following relations are valid

$$
\begin{aligned}
&\text{(a)} \quad \cos(\pi - \vartheta_0) = \sin\varphi \sin\delta + \cos\varphi \cos\delta \cos H \\
&\text{(b)} \quad \cos\varphi_0 = \frac{\cos(\pi - \vartheta_0)\sin\varphi - \sin\delta}{\sin(\pi - \vartheta_0)\cos\varphi}
\end{aligned}
\tag{1.11}
$$

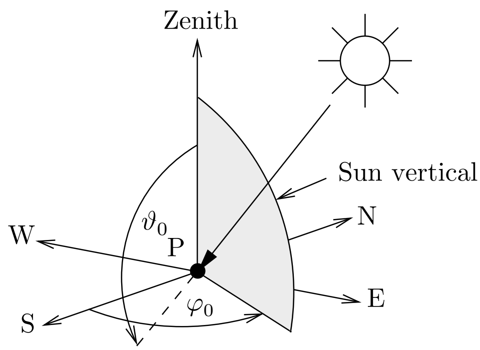

Fig. 1.10 Coordinates defining the position of the Sun.

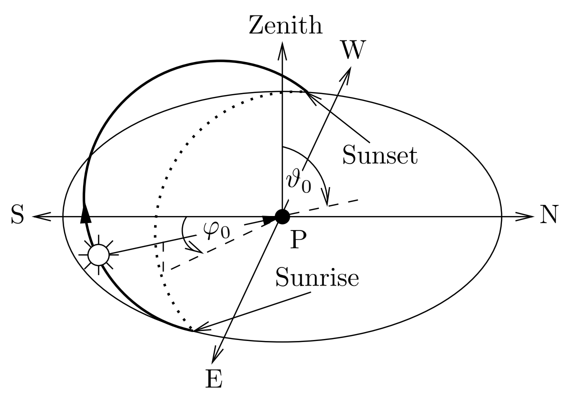

Fig. 1.11 Apparent solar track during the course of the day. The dotted curve marks the projection of the solar path onto the horizontal plane.

At solar noon at any latitude we have $H = 0$. In this case we obtain from (1.11a) $(\pi - \vartheta_0) = \varphi - \delta$. At sunrise or sunset at any latitude $\vartheta_0 = 90^\circ$ and $H = D_\mathrm{h}$. The term D_h is also called the *half-day length* since it is half the time interval between sunrise and sunset. Excepting the poles we find from (1.11a)

$$\cos D_\mathrm{h} = -\tan\varphi\tan\delta \tag{1.12}$$

At the equator on all days and at the equinoxes ($\delta = 0$) at all latitudes (with $\varphi \neq \pm 90^\circ$) we find $D_\mathrm{h} = 90^\circ$ or 6 h. The latitude of the *polar night* is found by setting in (1.12) $D_\mathrm{h} = 0$ so that $\tan\varphi = -\cot\delta$ (with $\delta \neq 0$) and $\varphi(\text{polar night}) = 90^\circ - |\delta|$ in the winter hemisphere.

The daily total solar radiation Q_s incident on a horizontal surface at the top of the atmosphere is found by integrating the incoming solar radiation over the length

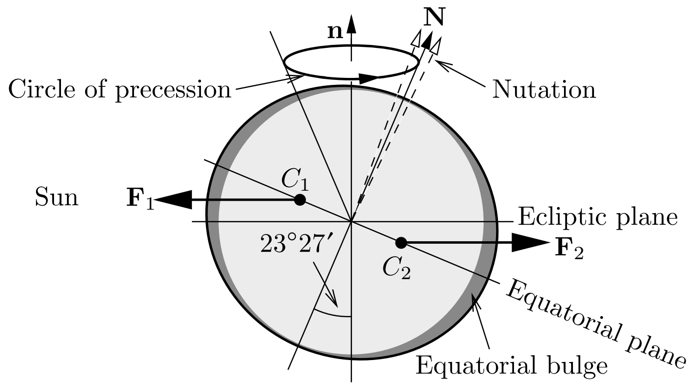

Fig. 1.12 Precession and nutation of the Earth.

of the day. Thus from (1.5) we find

$$Q_s = S_0 \left(\frac{a}{r(J)}\right)^2 \int_{-D_h}^{D_h} \cos(\pi - \vartheta_0) dt \tag{1.13}$$

Since the angular velocity of the Earth can be written as $\Omega = dH/dt = 2\pi$ day^{-1} we obtain from (1.11a) after some simple integration

$$Q_s = S_0 \left(\frac{a}{r(J)}\right)^2 \frac{86400}{\pi} (D_h \sin\varphi \sin\delta + \cos\varphi \cos\delta \sin D_h) \ \mathrm{J\,m^{-2} day^{-1}} \tag{1.14}$$

In the first term D_h must be expressed in radians. The expression $(a/r(J))^2$ never departs by more than about 3% from unity. Graphical representations of this formula are given in various texts, for example in Sellers (1965) where additional details may be found.

1.3.3 Long-term variations of the Earth's orbital parameters

For completeness we briefly discuss the most important variations of the Earth's orbit around the Sun. The *eccentricity e* of the Earth's elliptical orbit varies irregularly between 0 and 0.05 with its current value $e = 0.01673$. The period of this oscillation is approximately 100 000 years. The Earth's rotational axis **N** precesses around the normal of the ecliptic plane **n** with an angle of $23°27'$. The reason for the precession of the Earth is that it is not an ideal sphere, but it has the shape of a geoid, that is, the poles are flattened and an *equatorial bulge* of about 21 km is observed, see Figure 1.12. First we investigate the influence of the Sun on the geoidal form of the Earth. At the center of the Earth the gravitational attraction of the Sun and the centrifugal force due to the revolving motion of the Earth around the Sun are equal but opposite in sign. At the center of gravity C_1 (left half of the geoid) the attractional force of the Sun is larger than the centrifugal force, which is due to the smaller distance of C_1 to the Sun. At the center of gravity C_2 (right half of the geoid) we observe the opposite situation, which is due to the larger distance of C_2 to the Sun as compared to the center of the Earth; here the centrifugal force preponderates the attractional force of the Sun. Hence, at C_1 the resultant force $\mathbf{F}_1$ is directed toward the Sun whereas at C_2 the resultant force $\mathbf{F}_2$ is directed away from the Sun. Owing to the inclination of the ecliptic plane the forces $\mathbf{F}_1$ and $\mathbf{F}_2$ form a couple attempting to place the Earth's axis in the upright position. This results in the precession of the Earth's axis. The Moon, whose orbital plane nearly coincides with the orbital plane of the Earth, acts in the same way but even more effectively. Here, the small mass of the Moon in comparison with the mass of the Sun is overcompensated by the small distance between Moon and Earth. As a result of these forces, **N** revolves on the mantle of a cone as shown in Figure 1.12. The time for a full rotation around the *circle of precession* amounts to about 25 780 years.

Apart from the Sun and the Moon the other planets of the solar system also exert an influence on the inclination of the ecliptic leading to changes in ε between $21°55'$ and $24°18'$ having a period of about 40 000 years. Finally, in addition to the precession, the Earth's rotational axis exhibits also a nodding motion. This effect is caused by the fact that the Moon's gravitational influence varies in time. This *nutation* leads to a small variation of the Earth's axis inclination and has a period of about 18.6 years.

1.4 Basic definitions of radiative quantities

In this section we will present some basic definitions and the terminologies used in this book. The *photon* is considered to be an idealized infinitesimally small particle with zero rest mass carrying the energy

$$e(\nu) = h\nu \tag{1.15}$$

where $h = 6.626196 \times 10^{-34}$ J s is *Planck's constant*, and ν is the frequency of the electromagnetic radiation. Frequency units are Hertz (Hz) where 1 Hz is 1 cycle s^{-1}. Considering a single photon one may attribute to it a *momentum* $\mathbf{p}(\nu)$ with magnitude

$$p(\nu) = |\mathbf{p}(\nu)| = \frac{e(\nu)}{c} \tag{1.16}$$

where $c = 2.997925 \times 10^8$ m s^{-1} is the *vacuum speed of light*. Photons may travel in an arbitrary direction specified by the unit vector $\mathbf{\Omega}$. Therefore, the vectorial

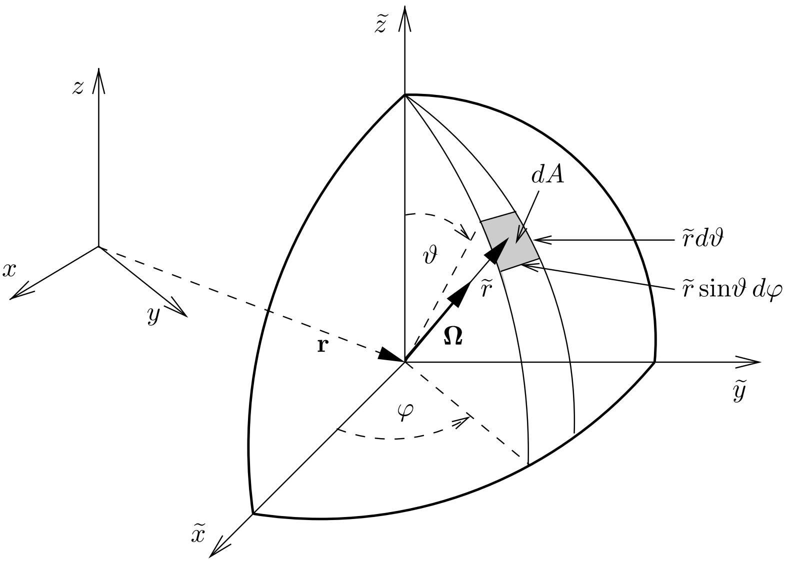

Fig. 1.13 Definition of the local spherical $(\tilde{r}, \vartheta, \varphi)$-coordinate system and the direction $\mathbf{\Omega}$.

notation of the photon's momentum can be expressed as

$$\mathbf{p}(\nu) = \frac{e(\nu)}{c}\mathbf{\Omega} = \frac{h\nu}{c}\mathbf{\Omega} \tag{1.17}$$

As soon as the photon interferes with matter, various types of interactions between the atoms of the material and the photon may occur. A single interaction may be an *absorption* or a *scattering process*. Between any two scattering interactions the photon is assumed to travel in a straight line with the speed of light c. We will also assume that during a scattering process the photon suffers no change in frequency. In this case one speaks of *elastic scattering*.

In some situations *inelastic scattering* might be of importance where in addition to the change of flight direction a shift in the photon's frequency occurs. One important example for atmospheric applications is *Raman scattering*. *Rayleigh scattering* and *Mie scattering* to be discussed later are examples of elastic scattering processes. Inelastic scattering processes will not be investigated in this book.

Six coordinates are required to unambiguously describe the photon at time t. These are the three coordinates of the position vector $\mathbf{r}$, the magnitude of momentum $p(\nu)$ and two angles characterizing the direction of flight $\mathbf{\Omega}$. At a certain point in space a local system of Cartesian coordinates $(\tilde{x}, \tilde{y}, \tilde{z})$ is introduced. At the origin of this system we define a spherical coordinate system $\tilde{r}$, ϑ, φ, where $\tilde{r}$ is the radial distance from the origin located at $\mathbf{r}$ and (ϑ, φ) are the zenith and azimuthal angle, respectively, see Figure 1.13. In the latter system the direction $\mathbf{\Omega}$ may be described

Table 1.1 *Definition of special radiance fields*

Radiance field	List of variables
Stationary	$I_\nu = I_\nu(\mathbf{r}, \mathbf{\Omega})$
Isotropic	$I_\nu = I_\nu(\mathbf{r}, t)$
Homogeneous	$I_\nu = I_\nu(\mathbf{\Omega}, t)$
Homogeneous and isotropic	$I_\nu = I_\nu(t)$

by the triple set of coordinates ($\tilde{r} = 1, \vartheta, \varphi$). The differential *solid angle element* $d\Omega$ is defined by

$$d\Omega = \frac{dA}{\tilde{r}^2} \tag{1.18}$$

Here, $dA = \tilde{r}^2 \sin\vartheta \, d\vartheta \, d\varphi$ is the differential area element on a sphere with radius $\tilde{r}$, see Figure 1.13. Thus we obtain

$$\boxed{d\Omega = \sin\vartheta \, d\vartheta \, d\varphi} \tag{1.19}$$

Integration over the unit sphere yields

$$\int_{4\pi} d\Omega = \int_0^{2\pi} \int_0^{\pi} \sin\vartheta \, d\vartheta \, d\varphi = \int_0^{2\pi} \int_{-1}^{1} d\mu \, d\varphi = 4\pi \tag{1.20}$$

where the abbreviation $\mu = \cos\vartheta$ has been introduced.

The *distribution function of photons* $f(\nu, \mathbf{r}, \mathbf{\Omega}, t) = f_\nu(\mathbf{r}, \mathbf{\Omega}, t)$ is defined by[2]

$$N_\nu(\mathbf{r}, \mathbf{\Omega}, t) d\nu = f_\nu(\mathbf{r}, \mathbf{\Omega}, t) \, dV \, d\Omega \, d\nu \tag{1.21}$$

where $N_\nu d\nu$ represents the number of photons at time t contained within the volume element dV centered at $\mathbf{r}$, within the solid angle element $d\Omega$ about the flight direction $\mathbf{\Omega}$, and within the frequency interval $(\nu, \nu + d\nu)$. Therefore, f_ν has units of ($\mathrm{m^{-3}\,sr^{-1}\,Hz^{-1}}$). In place of the photon distribution function f_ν, in radiative transfer theory it is customary to use the *radiance* $I_\nu(\mathbf{r}, \mathbf{\Omega}, t)$ as defined by

$$I_\nu(\mathbf{r}, \mathbf{\Omega}, t) = ch\nu f_\nu(\mathbf{r}, \mathbf{\Omega}, t) \tag{1.22}$$

From this equation it is seen that the monochromatic radiance is expressed in units of ($\mathrm{W\,m^{-2}\,sr^{-1}\,Hz^{-1}}$). In the most general case the radiance field is time dependent, it varies in space, direction, and frequency. Table 1.1 briefly lists some special cases of I_ν.

[2] The dependence of radiative quantities on frequency is commonly denoted by the subscript ν.

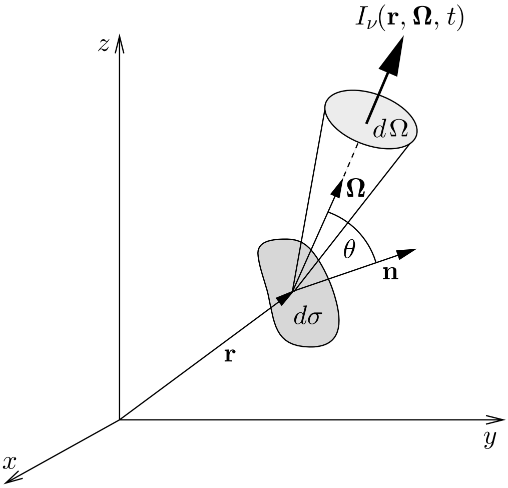

Fig. 1.14 Radiative energy streaming through the infinitesimal surface element $d\sigma$ with surface normal $\mathbf{n}$ into the solid angle element $d\Omega$ around the flight direction $\mathbf{\Omega}$ of the photons.

The physical meaning of the radiance can be illustrated with the help of the energy relation

$$u_\nu(\mathbf{r}, \mathbf{\Omega}, t)d\nu = I_\nu(\mathbf{r}, \mathbf{\Omega}, t)\cos\theta\, d\Omega\, d\sigma\, dt\, d\nu \tag{1.23}$$

Thus $u_\nu d\nu$ is the radiative energy contained within the frequency interval $(\nu, \nu + d\nu)$ streaming during dt at $\mathbf{r}$ through the surface element $d\sigma$ with unit surface normal $\mathbf{n}$ into the solid angle element $d\Omega$ along $\mathbf{\Omega}$. The angle between $\mathbf{\Omega}$ and the surface normal of $d\sigma$ is denoted by θ, see Figure 1.14. Therefore, $I_\nu d\nu$ is expressed in (W m^{-2} sr^{-1}).

The *energy density* $\hat{u}(\mathbf{r}, t)$ of the radiation field, expressed in units of (J m^{-3}), is obtained by integrating the term $h\nu f_\nu$ over all directions and frequencies

$$\boxed{\hat{u}(\mathbf{r}, t) = \int_0^\infty \int_{4\pi} h\nu f_\nu(\mathbf{r}, \mathbf{\Omega}, t)\, d\Omega\, d\nu = \frac{1}{c}\int_0^\infty \int_{4\pi} I_\nu(\mathbf{r}, \mathbf{\Omega}, t)\, d\Omega\, d\nu} \tag{1.24}$$

Let us now consider the important case that the radiance is described by the *Planck function* B_ν (W m^{-2} sr^{-1} Hz^{-1}), which is also known as the *spectral black body radiance*. This special radiation field which is stationary, isotropic and homogeneous coexists with matter in *perfect thermodynamic equilibrium* at temperature T. The expression

$$B_\nu d\nu = \frac{2h\nu^3}{c^2}(e^{h\nu/kT} - 1)^{-1} d\nu \tag{1.25}$$

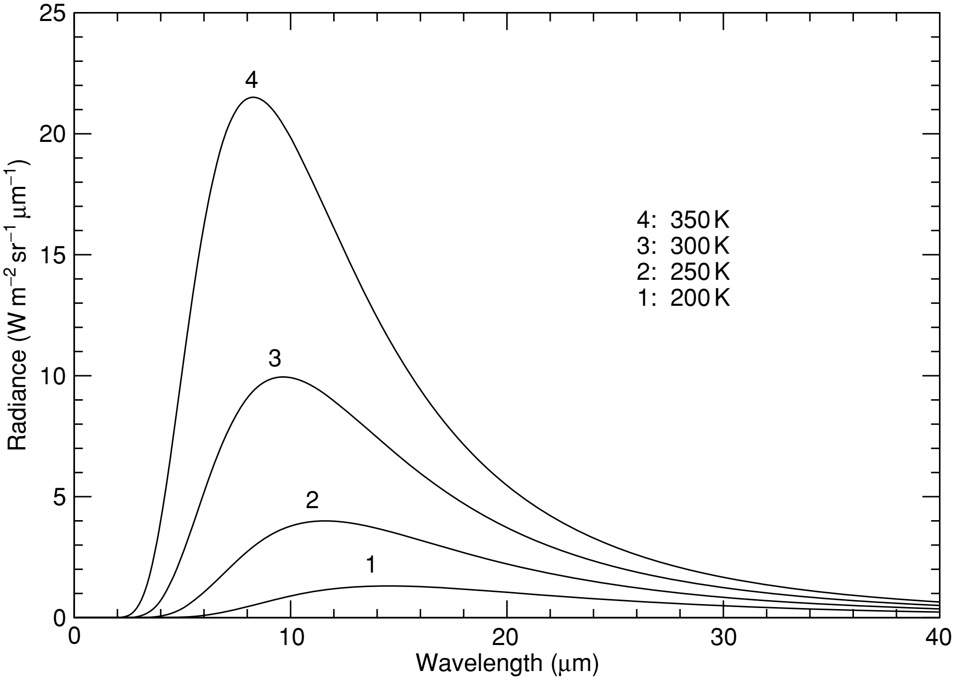

Fig. 1.15 Planckian black body curves for various temperatures.

represents the energy (unpolarized radiation) emitted by a black unit surface area per unit time interval within a cone of solid angle $\Omega_0 = 1$ sr vertical to the emitting surface in the frequency range between ν and $\nu + d\nu$.

Figure 1.15 depicts four Planck curves as function of the wavelength for the temperatures 200, 250, 300 and 350 K. It is clearly seen that with decreasing temperature the maxima of the curves are shifted towards larger wavelengths. This phenomenon is also known as *Wien's displacement law*. The Planck curve of a black body with temperature 6000 K (the Sun) has its maximum around 0.5 µm while for a black body with $T = 300$ K (the Earth) the maximum is found at 10 µm. For a further discussion of Wien's displacement law see also Problem 1.1.

The constant $k = 1.380662 \times 10^{-23}$ J K^{-1} appearing in (1.25) is known as the *Boltzmann constant*. The corresponding energy density follows from

$$\hat{u} = \frac{1}{c}\int_0^\infty \int_{4\pi} B_\nu d\Omega\, d\nu = \frac{4\pi}{c}\int_0^\infty \frac{2h\nu^3}{c^2}(e^{h\nu/kT} - 1)^{-1} d\nu \tag{1.26}$$

The integral over frequency can be evaluated by substituting the new variable $x = h\nu/kT$ and developing the exponential term $(e^x - 1)^{-1}$ into a power series,

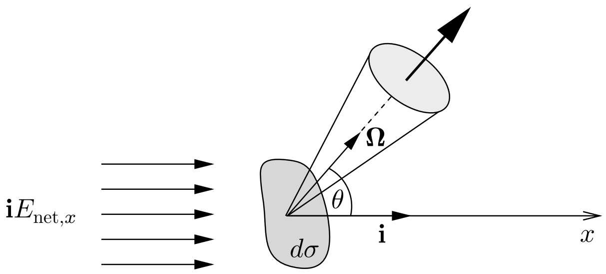

Fig. 1.16 Radiative energy streaming through the infinitesimal surface element $d\sigma$ in x-direction.

yielding

$$\hat{u} = \frac{8\pi k^4 T^4}{(hc)^3} \int_0^\infty x^3 (e^x - 1)^{-1} dx = \frac{48\pi (kT)^4}{(hc)^3} \sum_{n=1}^{\infty} \frac{1}{n^4} \tag{1.27}$$

Since

$$\sum_{n=1}^{\infty} \frac{1}{n^4} = \frac{\pi^4}{90} \tag{1.28}$$

the final result is

$$\boxed{\hat{u} = \frac{4}{c}\sigma T^4, \qquad \sigma = \frac{2\pi^5 k^4}{15 h^3 c^2} = 5.67032 \times 10^{-8}\ \mathrm{W\,m^{-2}\,K^{-4}}} \tag{1.29}$$

where σ is the *Stefan–Boltzmann constant*. Equation (1.29) can also be derived from purely thermodynamic arguments as shown, for example, in THD (2004).

1.5 The net radiative flux density vector

Consider the special case that $\mathbf{\Omega}$ is located in the (x, z)-plane and that the normal unit vector $\mathbf{n}$ of the surface element $d\sigma$ points in the x-direction of a Cartesian coordinate system, that is $\mathbf{n} = \mathbf{i}$. According to (1.23) for the spectral differential radiative energy crossing $d\sigma$ during dt we find the expression

$$\begin{aligned} E_{\mathrm{net},x,\nu}(\mathbf{r}, \mathbf{\Omega}, t) d\nu &= \frac{u_\nu(\mathbf{r}, \mathbf{\Omega}, t) d\nu}{d\sigma\, dt} = I_\nu(\mathbf{r}, \mathbf{\Omega}, t) \cos\theta \, d\Omega \, d\nu \\ &= I_\nu(\mathbf{r}, \mathbf{\Omega}, t) \Omega_x \, d\Omega \, d\nu \end{aligned} \tag{1.30}$$

where $\Omega_x = \mathbf{\Omega} \cdot \mathbf{i} = \cos\theta = \sin\vartheta$ is the projection of $\mathbf{\Omega}$ onto the x-axis, see Figures 1.16 and 1.17. Integrating this relation over the solid angle and over all

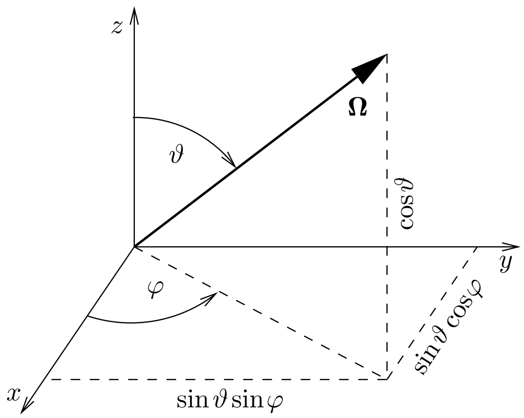

Fig. 1.17 Cartesian components of the unit vector $\mathbf{\Omega}$ pointing in the direction of photon travel.

frequencies yields the radiative energy streaming within unit time through the surface element in the x-direction

$$E_{\mathrm{net},x}(\mathbf{r},t)=\int_0^\infty\int_{4\pi}\Omega_x I_\nu(\mathbf{r},\mathbf{\Omega},t)d\Omega\,d\nu=\int_0^\infty\int_{4\pi}\Omega_x ch\nu f_\nu(\mathbf{r},\mathbf{\Omega},t)d\Omega\,d\nu \tag{1.31}$$

In the general case Ω_x will be a more complicated expression. If ($E_{\mathrm{net},x}$, $E_{\mathrm{net},y}$, $E_{\mathrm{net},z}$) are the three components of the *net radiative flux density vector*, then $\mathbf{E}_{\mathrm{net}}$ is given by

$$\boxed{\mathbf{E}_{\mathrm{net}}(\mathbf{r},t)=\int_0^\infty\int_{4\pi}\mathbf{\Omega} I_\nu(\mathbf{r},\mathbf{\Omega},t)d\Omega\,d\nu=\mathbf{i}E_{\mathrm{net},x}(\mathbf{r},t)+\mathbf{j}E_{\mathrm{net},y}(\mathbf{r},t)+\mathbf{k}E_{\mathrm{net},z}(\mathbf{r},t)} \tag{1.32}$$

where

$$\begin{aligned}E_{\mathrm{net},y}(\mathbf{r},t)&=\int_0^\infty\int_{4\pi}\Omega_y I_\nu(\mathbf{r},\mathbf{\Omega},t)d\Omega\,d\nu\\E_{\mathrm{net},z}(\mathbf{r},t)&=\int_0^\infty\int_{4\pi}\Omega_z I_\nu(\mathbf{r},\mathbf{\Omega},t)d\Omega\,d\nu\end{aligned} \tag{1.33}$$

We will now derive an explicit form of $\mathbf{E}_{\mathrm{net}}$ in Cartesian coordinates. From (1.32) follows the definition of the *spectral net radiative flux density vector*

$$\mathbf{E}_{\mathrm{net},\nu}(\mathbf{r},t)=\int_{4\pi}\mathbf{\Omega} I_\nu(\mathbf{r},\mathbf{\Omega},t)d\Omega \tag{1.34}$$

Thus the component of $\mathbf{E}_{\text{net},\nu}(\mathbf{r}, t)$ in the arbitrary direction $\mathbf{n}$ is given by

$$E_{\text{net},n,\nu}(\mathbf{r}, t) = \mathbf{E}_{\text{net},\nu}(\mathbf{r}, t) \cdot \mathbf{n} = \int_{4\pi} \mathbf{\Omega} \cdot \mathbf{n} I_\nu(\mathbf{r}, \mathbf{\Omega}, t) d\Omega = \int_{4\pi} \cos(\mathbf{\Omega}, \mathbf{n}) I_\nu(\mathbf{r}, \mathbf{\Omega}, t) d\Omega \tag{1.35}$$

To find the Cartesian components $(\Omega_x, \Omega_y, \Omega_z)$, of the unit vector $\mathbf{\Omega} = (1, \vartheta, \varphi)$ we perform the scalar multiplication with the Cartesian unit vectors $\mathbf{i}$, $\mathbf{j}$ and $\mathbf{k}$. From Figure 1.17 we find immediately

$$\begin{aligned} \mathbf{\Omega} \cdot \mathbf{i} = \Omega_x &= \cos(\mathbf{\Omega}, \mathbf{i}) = \sin\vartheta \cos\varphi \\ \mathbf{\Omega} \cdot \mathbf{j} = \Omega_y &= \cos(\mathbf{\Omega}, \mathbf{j}) = \sin\vartheta \sin\varphi \\ \mathbf{\Omega} \cdot \mathbf{k} = \Omega_z &= \cos(\mathbf{\Omega}, \mathbf{k}) = \cos\vartheta = \mu \end{aligned} \tag{1.36}$$

Thus, from (1.36) the Cartesian components of $\mathbf{E}_{\text{net},\nu}(\mathbf{r}, t)$ are finally given as

$$\boxed{\begin{aligned} &\text{(a)}\ \ E_{\text{net},x,\nu}(\mathbf{r}, t) = \int_0^{2\pi} \int_{-1}^{1} I_\nu(\mathbf{r}, \mu, \varphi, t) \cos\varphi (1-\mu^2)^{1/2} d\mu\, d\varphi \\ &\text{(b)}\ \ E_{\text{net},y,\nu}(\mathbf{r}, t) = \int_0^{2\pi} \int_{-1}^{1} I_\nu(\mathbf{r}, \mu, \varphi, t) \sin\varphi (1-\mu^2)^{1/2} d\mu\, d\varphi \\ &\text{(c)}\ \ E_{\text{net},z,\nu}(\mathbf{r}, t) = \int_0^{2\pi} \int_{-1}^{1} I_\nu(\mathbf{r}, \mu, \varphi, t) \mu\, d\mu\, d\varphi \end{aligned}} \tag{1.37}$$

with $(1-\mu^2)^{1/2} = \sin\vartheta$ and $d\Omega = -d\mu d\varphi$.

It is straightforward to show that for an isotropic radiation field $\mathbf{E}_{\text{net},\nu} = 0$. For example, evaluating in (1.37a) for $I_\nu = const$ the integral of the x-component yields

$$\int_0^{2\pi} \cos\varphi \int_{-1}^{1} (1-\mu^2)^{1/2} d\mu\, d\varphi = \int_{4\pi} \Omega_x d\Omega = 0 \tag{1.38}$$

Similarly we obtain for the integrals of the y- and z-component

$$\int_{4\pi} \Omega_y d\Omega = 0, \quad \int_{4\pi} \Omega_z d\Omega = 0 \tag{1.39}$$

1.6 The interaction of radiation with matter

1.6.1 Absorption

If a photon travels through space filled with matter, a certain *absorption probability* can be defined. For the mathematical description of this process the *absorption coefficient* $k_{\text{abs},\nu}(\mathbf{r}, t)$ with units (m^{-1}) is introduced. The dimensionless differential

$$\boxed{d\tau_{\text{abs}}(\mathbf{r}, t) = k_{\text{abs},\nu}(\mathbf{r}, t)\, ds} \tag{1.40}$$

is the so-called *differential optical depth for absorption* where ds is the geometrical distance travelled by the photon. Thus the differential $d\tau_{\mathrm{abs}}(\mathbf{r}, t)$ is a measure for the probability that the photon is absorbed along ds so that the photon disappears. It is important to realize that (1.40) is valid only for *isotropic media*. In general, for *anisotropic media*, the absorption coefficient not only depends on position, frequency and time but also on the direction $\boldsymbol{\Omega}$. For all practical purposes, the atmosphere can be considered an isotropic medium.

Sometimes it is preferable to use the *mass absorption coefficient* $\kappa_{\mathrm{abs},\nu}(\mathbf{r}, t)$ which is defined by the relation

$$\boxed{k_{\mathrm{abs},\nu}(\mathbf{r}, t) = \rho_{\mathrm{abs}}(\mathbf{r}, t)\kappa_{\mathrm{abs},\nu}(\mathbf{r}, t)} \tag{1.41}$$

where $\rho_{\mathrm{abs}}(\mathbf{r}, t)$ is the density of the absorbing medium, and $\kappa_{\mathrm{abs}}(\mathbf{r}, t)$ has units of $(\mathrm{m}^2\,\mathrm{kg}^{-1})$.

1.6.2 Scattering

In a similar manner the photon may suffer an elastic scattering process after having travelled a certain distance ds. The occurrence of a scattering process does not mean that the photon disappears at the location of scattering, instead of that it changes its flight direction from $\boldsymbol{\Omega}'$ to $\boldsymbol{\Omega}$. Let us denote the *differential scattering coefficient* by $k_{\mathrm{sca},\nu}(\mathbf{r}, \boldsymbol{\Omega}' \to \boldsymbol{\Omega}, t)$. In analogy to (1.40), the *differential optical depth for scattering* is defined as

$$\boxed{d\tau_{\mathrm{sca}}(\mathbf{r}, \boldsymbol{\Omega}' \to \boldsymbol{\Omega}, t) = k_{\mathrm{sca},\nu}(\mathbf{r}, \boldsymbol{\Omega}' \to \boldsymbol{\Omega}, t)\, d\Omega\, ds} \tag{1.42}$$

This expression is a measure of the probability that a photon of frequency ν with initial direction $\boldsymbol{\Omega}'$, in traveling the distance ds, is scattered into $d\Omega$ having the new direction $\boldsymbol{\Omega}$. From (1.42) it is clear that $k_{\mathrm{sca},\nu}(\mathbf{r}, \boldsymbol{\Omega}' \to \boldsymbol{\Omega}, t)$ is expressed in units of $(\mathrm{m}^{-1}\,\mathrm{sr}^{-1})$. It is noteworthy that the differential scattering coefficient agrees with the *scattering function* $\tilde{\mathcal{P}}(\cos\Theta)$ which will be introduced in a later chapter. The notation $\boldsymbol{\Omega}' \to \boldsymbol{\Omega}$ has been chosen since in general the differential scattering probability depends explicitly on both directions $\boldsymbol{\Omega}'$ and $\boldsymbol{\Omega}$. However, for applications involving homogeneous spherical particles (e.g. cloud droplets) it is obvious that the scattering process depends only on the cosine of the *scattering angle*

$$\boxed{\cos\Theta = \boldsymbol{\Omega}' \cdot \boldsymbol{\Omega}} \tag{1.43}$$

This means that scattering is rotationally symmetric about the direction of incidence, see Figure 1.18. In case of randomly oriented inhomogeneous or non-spherical

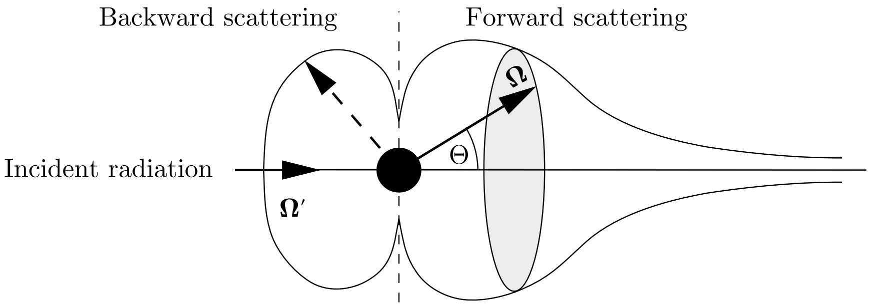

Fig. 1.18 Illustration of the rotationally symmetric scattering phase function. $\mathcal{P}(\mathbf{r}, \boldsymbol{\Omega}' \rightarrow \boldsymbol{\Omega}) = const$ on the circle defined by all points with $\Theta = const$.

particles (e.g. ice particles or aerosol particles) it is often assumed that the scattering angle may be defined analogously.

If we integrate the differential scattering coefficient over all possible directions $\boldsymbol{\Omega}$, we obtain the ordinary scattering coefficient $k_{\text{sca},\nu}(\mathbf{r}, t)$

$$k_{\text{sca},\nu}(\mathbf{r}, t) = \int_{4\pi} k_{\text{sca},\nu}(\mathbf{r}, \boldsymbol{\Omega}' \rightarrow \boldsymbol{\Omega}, t) d\Omega \tag{1.44}$$

This relation together with (1.42) can be used to define the *scattering phase function* or simply *phase function* $\mathcal{P}_\nu(\mathbf{r}, \boldsymbol{\Omega}' \rightarrow \boldsymbol{\Omega}, t)$

$$\boxed{k_{\text{sca},\nu}(\mathbf{r}, \boldsymbol{\Omega}' \rightarrow \boldsymbol{\Omega}, t) = \frac{1}{4\pi} k_{\text{sca},\nu}(\mathbf{r}, t) \mathcal{P}_\nu(\mathbf{r}, \boldsymbol{\Omega}' \rightarrow \boldsymbol{\Omega}, t)} \tag{1.45}$$

The scattering phase function is a measure of the probability density distribution for a scattering process from the incident direction $\boldsymbol{\Omega}'$ into the direction $\boldsymbol{\Omega}$. The normalization of $\mathcal{P}$ is guaranteed since integrating (1.45) over the unit sphere, utilizing (1.44), yields

$$\frac{1}{4\pi} \int_{4\pi} \mathcal{P}_\nu(\mathbf{r}, \boldsymbol{\Omega}' \rightarrow \boldsymbol{\Omega}, t) d\Omega = 1 \tag{1.46}$$

It is instructive to discuss a particularly simple form of scattering, namely an *isotropic scattering process*. In this case the phase function is simply given by

$$\mathcal{P}_\nu(\mathbf{r}, \boldsymbol{\Omega}' \rightarrow \boldsymbol{\Omega}, t) = 1 \tag{1.47}$$

i.e. for each direction there is equal probability of scattering.

The sum of absorption and scattering is called extinction. The *extinction coefficient* is defined by

$$\boxed{k_{\text{ext},\nu}(\mathbf{r}, t) = k_{\text{abs},\nu}(\mathbf{r}, t) + k_{\text{sca},\nu}(\mathbf{r}, t)} \tag{1.48}$$

Another important optical parameter is the *single scattering albedo* $\omega_{0,\nu}(\mathbf{r}, t)$ which is defined as the relative amount of scattering involved in the extinction process

$$\boxed{\omega_{0,\nu}(\mathbf{r}, t) = \frac{k_{\mathrm{sca},\nu}(\mathbf{r}, t)}{k_{\mathrm{ext},\nu}(\mathbf{r}, t)} = 1 - \frac{k_{\mathrm{abs},\nu}(\mathbf{r}, t)}{k_{\mathrm{ext},\nu}(\mathbf{r}, t)}} \tag{1.49}$$

Of particular importance is the case $\omega_{0,\nu}(\mathbf{r}, t) = 1$ for which the scattering process is *conservative*. In a medium with conservative scattering no absorption of radiation occurs. Later it will be shown that a conservative plane-parallel medium is characterized by a vertically constant net radiative flux density.

1.6.3 Emission

Emission is a process that generates photons within the medium. In the long-wave spectral region photons are emitted and absorbed by atmospheric trace gases such as water vapor, carbon dioxide, ozone, by cloud and aerosol particles, and by the Earth's surface. As already mentioned previously, in case of local thermodynamic equilibrium these emission processes can be described by the Planckian function.

For the mathematical formulation of emission processes we introduce the so-called *emission coefficient* $j_\nu(\mathbf{r}, t)$ for isotropic radiation sources. This coefficient defines the number of photons emitted per unit time and unit volume within the frequency interval $(\nu, \nu + d\nu)$. The photons are contained in the solid angle element $d\boldsymbol{\Omega} = \boldsymbol{\Omega}\, d\Omega$

$$\boxed{\frac{\partial}{\partial t} N_\nu(\mathbf{r}, t)\Big|_{\mathrm{em}} = j_\nu(\mathbf{r}, t)\, dV\, d\Omega\, d\nu} \tag{1.50}$$

The emission coefficient is expressed in units of $(\mathrm{m}^{-3}\,\mathrm{s}^{-1}\,\mathrm{sr}^{-1}\,\mathrm{Hz}^{-1})$.

1.7 Problems

1.1: With increasing temperature the maximum of the Planckian black body curve is shifted to shorter wavelengths. Observing that $d\nu = -c\,d\lambda/\lambda^2$, express (1.25) in terms of wavelength.

(a) Differentiate Planck's law with respect to wavelength and estimate the wavelength $\lambda_{\max}$ of maximum emission for a fixed temperature T. The resulting formula is known as Wien's displacement law.

(b) Find $\lambda_{\max}$ for the solar temperature $T = 6000$ K and for the terrestrial temperature $T = 300$ K.

1.2: Calculate for the two asymptotic situations

(a) $\nu \ll 1$: *Rayleigh–Jeans distribution*
(b) $\nu \gg 1$: *Wien distribution*

the resulting simplified radiation laws of Planck.

1.3: Integrate Planck's formula (1.25) over all frequencies and directions to find the hemispheric flux density $E_{\mathrm{b}} = \sigma T^4$. This is known as the *Stefan–Boltzmann law*.

1.4: A black horizontal receiving element (radiometer) of unit area is located directly below the center of a circular cloud at height z having the temperature T_c. The cloud radius is R. Find an expression for the flux density E incident on the receiving element in terms of the Stefan–Boltzmann law, z and R. Assume that the cloud is a black body radiator whose radiance is $\sigma T^4/\pi$. Ignore any interactions of the radiation with the atmosphere.

(a) Start your analysis using Lambert's law of photometry.
(b) Rework the problem using equation (1.37c).

1.5: An idealized valley may be considered as the interior part of a spherical surface of radius a. The valley surface is assumed to radiate as a black body of temperature T.

(a) Find an expression for the radiation received by a radiometer which is located at a distance $z > a$ above the lowest part of the valley. Ignore any interaction of the radiation with the atmosphere.
(b) Repeat the calculation with the radiometer located below the center of curvature, that is $z < a$.

Hint: Use Lambert's law of photometry, see Problem 1.4.

1.6: A spherical emitter of radius a emits isotropically radiation into empty space.

(a) Find the flux density $\mathbf{E}_r = E_r(\mathbf{r})\mathbf{e}_r$ at a distance $r \geq a$ from the center of the sphere. $\mathbf{e}_r$ is a unit vector along the radius.
(b) From $\mathbf{E}_r$ obtain the power ϕ emitted by the sphere.
(c) Find the energy density $\hat{u}(\mathbf{r})$.

1.7: For a monochromatic homogeneous plane parallel radiation field (solar radiation $S_{0,\nu}$) find the energy density $\hat{u}_\nu$ and the net flux density $\mathbf{E}_{\mathrm{net},\nu}$. Ignore any interaction of the radiation with the atmosphere.

2

The radiative transfer equation

2.1 Eulerian derivation of the radiative transfer equation

In the following section we will derive a *budget equation for photons* in a medium in which scattering, absorption and emission processes take place. The photon budget equation finally results in the so-called *radiative transfer equation* (RTE) which is a linear integro-differential equation for the radiance $I_\nu(\mathbf{r}, \mathbf{\Omega}, t)$. Let us consider a six-dimensional (6-D) volume element in $(x, y, z, \vartheta, \varphi, \nu)$-space with side lengths $(\Delta x, \Delta y, \Delta z, \Delta\vartheta, \Delta\varphi, \Delta\nu)$. This volume element is assumed to be fixed in time t. According to (1.21), at point $\mathbf{r}$ the total number of photons N_ν is given by

$$N_\nu(\mathbf{r}, \mathbf{\Omega}, t) = f_\nu(\mathbf{r}, \mathbf{\Omega}, t)\Delta V \Delta\Omega\Delta\nu \tag{2.1}$$

where $\Delta V = \Delta x \Delta y \Delta z$ is the ordinary volume element in space. In order to simplify the notation, the dependence of different variables on $(\mathbf{r}, \mathbf{\Omega}, t)$ will henceforth be omitted except where confusion is likely to occur.

The derivation of the photon budget equation requires the knowledge of the local time rate of change of the number of photons leaving and entering the 6-D volume element

$$\frac{\partial N_\nu}{\partial t} = \frac{\partial f_\nu}{\partial t}\Delta V \Delta\Omega\Delta\nu \tag{2.2}$$

This change consists of the following processes.

$\left.\dfrac{\partial N_\nu}{\partial t}\right|_{\text{exch}}$: Exchange of photons of the considered volume element with the exterior surrounding.

$\left.\dfrac{\partial N_\nu}{\partial t}\right|_{\text{abs}}$: Absorption of photons with frequency ν and direction $\mathbf{\Omega}$.

$\left.\dfrac{\partial N_\nu}{\partial t}\right|_{\text{outsc}}$: Scattering of photons with frequency ν and direction $\mathbf{\Omega}$ into all other directions $\mathbf{\Omega}'$ (*outscattering*).

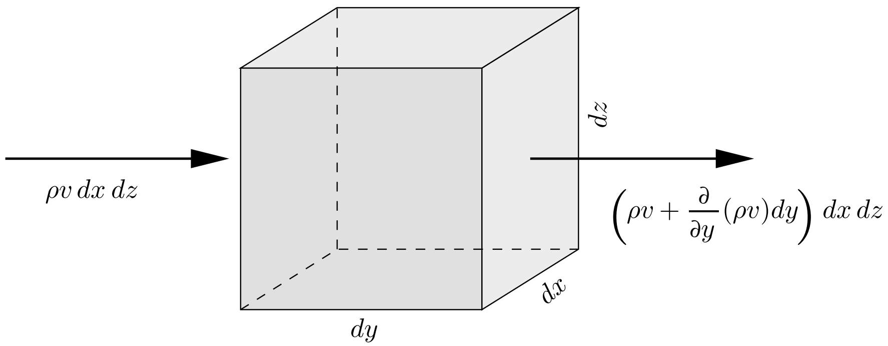

Fig. 2.1 Mass flux entering the left face and leaving the right face of a cube with volume $dx\, dy\, dz$.

$\left.\frac{\partial N_\nu}{\partial t}\right|_{\text{insc}}$: Scattering of photons with frequency ν and arbitrary direction $\mathbf{\Omega}'$ into the desired direction $\mathbf{\Omega}$ (*inscattering*).

$\left.\frac{\partial N_\nu}{\partial t}\right|_{\text{em}}$: Emission of photons with frequency ν in direction $\mathbf{\Omega}$.

The individual contributions of these processes to the photon budget equation will now be discussed in detail.

2.1.1 The exchange of photons

The exchange of photons can be treated in analogy to the *continuity equation for the mass* in fluid mechanics. We will consider a cube with side lengths (dx, dy, dz). The velocity of a fluid particle is given by $\mathbf{v} = u\mathbf{i} + v\mathbf{j} + w\mathbf{k}$, and ρ is the mass density of the medium. The volume dV is assumed to be fixed in space. The local time rate of change of the mass $dM = \rho\, dx\, dy\, dz$ of the cube is given by adding all mass fluxes through its surface. Figure 2.1 depicts the mass fluxes entering and leaving the infinitesimal volume element $dx\, dy\, dz$ through the vertical sides with area $dx\, dz$. Thus the net flux in y-direction is given by

$$F_{\rho,y} = -\left(\rho v + \frac{\partial}{\partial y}(\rho v) dy\right) dx\, dz + \rho v\, dx\, dz = -\frac{\partial}{\partial y}(\rho v) dx\, dy\, dz \tag{2.3}$$

In a similar manner we obtain the net fluxes $F_{\rho,x}$ and $F_{\rho,z}$ in the x- and z-direction. Adding up all three contributions and dividing by $dx\, dy\, dz$ yields the well-known continuity equation

$$\boxed{\frac{\partial \rho}{\partial t} = -\nabla \cdot (\rho \mathbf{v})} \tag{2.4}$$

The concept of obtaining the continuity equation for the mass M will now be applied to the derivation of the photon budget equation. The velocity of a photon is given by

$$\mathbf{v} = c\boldsymbol{\Omega} = c(\Omega_x \mathbf{i} + \Omega_y \mathbf{j} + \Omega_z \mathbf{k}) \tag{2.5}$$

Analogously to (2.3) the net flux of photons in the y-direction through the 6-D volume element $\Delta V \Delta\Omega \Delta\nu$ can be expressed by means of

$$F_{y,\nu} = -\frac{\partial}{\partial y}\left(c\Omega_y f_\nu\right) \Delta V \Delta\Omega \Delta\nu \tag{2.6}$$

Note that $F_{y,\nu}$ is expressed in units of (s^{-1}). Adding up the contributions of the three directions yields the time rate of change for the number of photons due to the exchange with the surroundings

$$\boxed{\left.\frac{\partial N_\nu}{\partial t}\right|_{\mathrm{exch}} = -\left(\frac{\partial}{\partial x}(\Omega_x f_\nu) + \frac{\partial}{\partial y}(\Omega_y f_\nu) + \frac{\partial}{\partial z}(\Omega_z f_\nu)\right) c\Delta V \Delta\Omega \Delta\nu} \tag{2.7}$$

The exchange term has been derived under the assumption that the medium's *index of refraction* is constant in space and time. This assumption is sufficient for most atmospheric applications. Otherwise, the photon path will be subject to refraction leading to photon trajectories which are curved in space.

2.1.2 The absorption of photons

The absorption rate of photons within the 6-D volume element is given by the product of the photon number N_ν and the probability that a photon will be absorbed during the time interval $(t, t + dt)$. Dividing (1.40) by dt yields

$$\frac{d\tau_{\mathrm{abs}}}{dt} = k_{\mathrm{abs},\nu}\frac{ds}{dt} = k_{\mathrm{abs},\nu} c \tag{2.8}$$

with $c = ds/dt$. Hence, for the total absorption rate of photons we obtain the expression

$$\boxed{\left.\frac{\partial N_\nu}{\partial t}\right|_{\mathrm{abs}} = N_\nu \frac{d\tau_{\mathrm{abs}}}{dt} = f_\nu k_{\mathrm{abs},\nu} c\Delta V \Delta\Omega \Delta\nu} \tag{2.9}$$

2.1.3 The scattering of photons

Figure 2.2 illustrates the inscattering and outscattering process of photons. For inscattering the direction of the photons is indicated by solid arrows, outscattering is denoted by dashed arrows. It will be noticed that for the direction $\boldsymbol{\Omega}$ inscattering represents a gain of photons whereas outscattering results in a reduction of the number of photons in this particular direction.

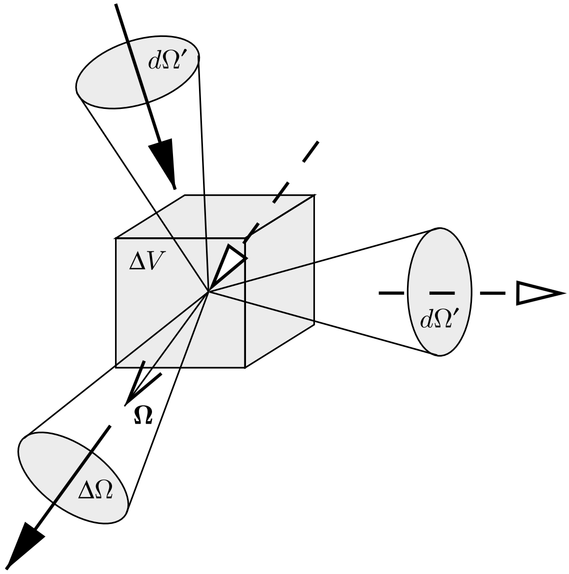

Fig. 2.2 Schematic view of the inscattering (solid arrows) and the outscattering (dashed arrows) processes.

Analogously to (1.42) we may express the probability that at time t a photon is scattered from $\mathbf{\Omega} \to \mathbf{\Omega}'$ by means of

$$d\tau_{\text{sca}}(\mathbf{\Omega} \to \mathbf{\Omega}') = k_{\text{sca},\nu}(\mathbf{\Omega} \to \mathbf{\Omega}')d\Omega' ds \tag{2.10}$$

Dividing this equation by dt and multiplying by the number of photons N_ν yields the time rate of change of photons resulting from the outscattering process $\mathbf{\Omega} \to \mathbf{\Omega}'$

$$N_\nu \frac{d}{dt}\left[\tau_{\text{sca}}(\mathbf{\Omega} \to \mathbf{\Omega}')\right] = N_\nu k_{\text{sca},\nu}(\mathbf{\Omega} \to \mathbf{\Omega}')d\Omega' c \tag{2.11}$$

The total loss of photons due to outscattering is obtained by integrating (2.11) over all directions $\mathbf{\Omega}'$

$$\begin{aligned}\left.\frac{\partial N_\nu}{\partial t}\right|_{\text{outsc}} &= N_\nu c \int_{4\pi} k_{\text{sca},\nu}(\mathbf{\Omega} \to \mathbf{\Omega}')d\Omega' \\ &= f_\nu \Delta V \Delta\Omega \Delta\nu \frac{c}{4\pi} \int_{4\pi} k_{\text{sca},\nu} \mathcal{P}_\nu(\mathbf{\Omega} \to \mathbf{\Omega}')d\Omega'\end{aligned} \tag{2.12}$$

Here, use was made of (1.45) and (2.1). Utilizing the normalization condition for the *phase function*

$$\frac{1}{4\pi} \int_{4\pi} \mathcal{P}_\nu(\mathbf{\Omega} \to \mathbf{\Omega}')d\Omega' = 1 \tag{2.13}$$

finally gives

$$\boxed{\left.\frac{\partial N_\nu}{\partial t}\right|_{\text{outsc}} = f_\nu k_{\text{sca},\nu} c \Delta V \Delta\Omega \Delta\nu} \tag{2.14}$$

In a similar manner we may find the gain of photons for the direction $\mathbf{\Omega}$ due to inscattering from all directions $\mathbf{\Omega}'$. The number of photons moving in direction $\mathbf{\Omega}'$, before inscattering takes place, is $f_\nu(\mathbf{r}, \mathbf{\Omega}', t)\,\Delta V d\Omega' \Delta\nu$. In analogy to (2.11) we have

$$N_\nu \frac{d}{dt}\left[\tau_{\text{sca}}(\mathbf{\Omega}' \rightarrow \mathbf{\Omega})\right] = f_\nu(\mathbf{\Omega}')\,\Delta V d\Omega' \Delta\nu k_{\text{sca},\nu}(\mathbf{\Omega}' \rightarrow \mathbf{\Omega})\Delta\Omega\, c \tag{2.15}$$

Integrating over all directions $\mathbf{\Omega}'$, using equation (1.45), we find for the inscattering rate

$$\boxed{\left.\frac{\partial N_\nu}{\partial t}\right|_{\text{insc}} = k_{\text{sca},\nu} \Delta V \Delta\Omega \Delta\nu \frac{c}{4\pi} \int_{4\pi} \mathcal{P}_\nu(\mathbf{\Omega}' \rightarrow \mathbf{\Omega}) f_\nu(\mathbf{\Omega}') d\Omega'} \tag{2.16}$$

2.1.4 The emission rate

Finally, according to (1.50) the time rate of change of photons due to *emission* is given by

$$\boxed{\left.\frac{\partial N_\nu}{\partial t}\right|_{\text{em}} = j_\nu\, \Delta V\, \Delta\Omega\, \Delta\nu} \tag{2.17}$$

Now we have derived mathematical expressions for the five contributions for the photon budget equation as listed at the beginning of this section.

2.1.5 The budget equation of the photon distribution function

The budget equation for the photon distribution function f_ν is obtained by adding up the individual contributions. Considering absorption and outscattering processes as negative contributions, we may write

$$\frac{\partial N_\nu}{\partial t} = \left.\frac{\partial N_\nu}{\partial t}\right|_{\text{exch}} - \left.\frac{\partial N_\nu}{\partial t}\right|_{\text{abs}} - \left.\frac{\partial N_\nu}{\partial t}\right|_{\text{outsc}} + \left.\frac{\partial N_\nu}{\partial t}\right|_{\text{insc}} + \left.\frac{\partial N_\nu}{\partial t}\right|_{\text{em}} \tag{2.18}$$

Combination of (2.7), (2.9), (2.14), (2.16), and (2.17) gives

$$\begin{aligned}\frac{\partial f_\nu}{\partial t} = &-c\left(\frac{\partial}{\partial x}(\Omega_x f_\nu) + \frac{\partial}{\partial y}(\Omega_y f_\nu) + \frac{\partial}{\partial z}(\Omega_z f_\nu)\right) - c f_\nu k_{\text{abs},\nu} - c f_\nu k_{\text{sca},\nu} \\ &+\frac{c}{4\pi} k_{\text{sca},\nu} \int_{4\pi} \mathcal{P}_\nu(\mathbf{\Omega}' \rightarrow \mathbf{\Omega}) f_\nu(\mathbf{\Omega}') d\Omega' + j_\nu \end{aligned} \tag{2.19}$$

where the common factor $\Delta V\, \Delta\Omega\, \Delta\nu$ has been cancelled out.

Obviously, the unit vector $\mathbf{\Omega}$ is divergence-free, that is

$$\nabla \cdot \mathbf{\Omega} = \frac{\partial \Omega_x}{\partial x} + \frac{\partial \Omega_y}{\partial y} + \frac{\partial \Omega_z}{\partial z} = 0 \tag{2.20}$$

Therefore, the streaming term on the right-hand side of (2.19) may further be simplified yielding the final form of the photon budget equation for a nonstationary situation

$$\frac{\partial f_\nu}{\partial t} = -c\mathbf{\Omega} \cdot \nabla f_\nu - c f_\nu k_{\text{ext},\nu} + \frac{c}{4\pi} k_{\text{sca},\nu} \int_{4\pi} \mathcal{P}_\nu(\mathbf{\Omega}' \to \mathbf{\Omega}) f_\nu(\mathbf{\Omega}') d\Omega' + j_\nu \tag{2.21}$$

Here, the extinction coefficient $k_{\text{ext},\nu}$ as defined in (1.48) has been introduced.

Since we consider the spatial change of the photon distribution function along ds in $\mathbf{\Omega}$-direction, ∇f_ν may be expressed in terms of

$$\nabla f_\nu = \mathbf{\Omega} \frac{d f_\nu}{ds} \tag{2.22}$$

so that

$$\mathbf{\Omega} \cdot \nabla f_\nu = \frac{d f_\nu}{ds} = \Omega_x \frac{\partial f_\nu}{\partial x} + \Omega_y \frac{\partial f_\nu}{\partial y} + \Omega_z \frac{\partial f_\nu}{\partial z} \tag{2.23}$$

According to (1.36) the Cartesian components of $\mathbf{\Omega}$ are given by

$$\Omega_x = \mathbf{\Omega} \cdot \mathbf{i} = \sin\vartheta \cos\varphi, \qquad \Omega_y = \mathbf{\Omega} \cdot \mathbf{j} = \sin\vartheta \sin\varphi, \qquad \Omega_z = \mathbf{\Omega} \cdot \mathbf{k} = \cos\vartheta \tag{2.24}$$

By introducing into (2.21) the radiance I_ν as defined in (1.22), one obtains the general *nonstationary form of the radiative transfer equation*

$$\boxed{\frac{1}{c}\frac{\partial I_\nu}{\partial t} + \mathbf{\Omega} \cdot \nabla I_\nu = -\, k_{\text{ext},\nu} I_\nu + \frac{k_{\text{sca},\nu}}{4\pi} \int_{4\pi} \mathcal{P}_\nu(\mathbf{\Omega}' \to \mathbf{\Omega}) I_\nu(\mathbf{\Omega}') d\Omega' + J_\nu^{\text{e}}} \tag{2.25}$$

Here, the *source function for true emission*

$$\boxed{J_\nu^{\text{e}}(\mathbf{r}, t) = h\nu j_\nu(\mathbf{r}, t)} \tag{2.26}$$

has been introduced. This function has units of (W m^{-3} sr^{-1} Hz^{-1}). Its relation to the *Planck function* will be described later.

For most atmospheric applications the term $1/c(\partial I/\partial t)$ in the RTE can be neglected in comparison to the remaining terms since the propagation speed c is very high. Thus (2.25) simplifies to

$$\mathbf{\Omega} \cdot \nabla I_\nu = -k_{\text{ext},\nu} I_\nu + \frac{k_{\text{sca},\nu}}{4\pi} \int_{4\pi} \mathcal{P}_\nu(\mathbf{\Omega}' \to \mathbf{\Omega}) I_\nu(\mathbf{\Omega}') d\Omega' + J_\nu^{\text{e}} \tag{2.27}$$

In the following we will assume that scattering takes place on spherical particles. Since according to (1.43) in this case the scattering process $\boldsymbol{\Omega}' \to \boldsymbol{\Omega}$ depends on the cosine of the scattering angle $\cos\Theta = \boldsymbol{\Omega}' \cdot \boldsymbol{\Omega}$ only, henceforth the term $\boldsymbol{\Omega}' \to \boldsymbol{\Omega}$ will be replaced by $\boldsymbol{\Omega}' \cdot \boldsymbol{\Omega}$ or by $\cos\Theta$. Utilizing in (2.27) the definition of the *single scattering albedo* as given in (1.49), we obtain the standard form of the RTE for a three-dimensional medium

$$\boxed{-\frac{1}{k_{\mathrm{ext},\nu}}\boldsymbol{\Omega} \cdot \nabla I_\nu = I_\nu - \frac{\omega_{0,\nu}}{4\pi}\int_{4\pi} \mathcal{P}_\nu(\boldsymbol{\Omega}' \cdot \boldsymbol{\Omega}) I_\nu(\boldsymbol{\Omega}')d\Omega' - \frac{1}{k_{\mathrm{ext},\nu}} J_\nu^{\mathrm{e}}} \tag{2.28}$$

The derivation of the RTE is based on arguments of radiation hydrodynamics as presented by Pomraning (1973) where many additional and interesting details may be found. The RTE can also be derived on the basis of geometric reasoning in the manner described by Chandrasekhar (1960).

In passing we would like to remark that the RTE is part of the atmospheric predictive system. With changing composition of the atmospheric constituents the radiation parameters are also changing so that radiance continues to be a function of time.

2.2 The direct–diffuse splitting of the radiance field

The *total solar radiation field* is defined as the sum of the *direct solar beam* and the *diffuse solar radiation*. Usually one writes the RTE (2.28) in a different form by splitting $I_\nu(\mathbf{r}, \boldsymbol{\Omega})$ into the unscattered direct light $S_\nu(\mathbf{r})$ and the diffuse light $I_{\mathrm{d},\nu}(\mathbf{r}, \boldsymbol{\Omega})$

$$I_\nu = I_{\mathrm{d},\nu} + S_\nu \delta(\boldsymbol{\Omega} - \boldsymbol{\Omega}_0) \tag{2.29}$$

where δ is the Dirac δ-function and $\boldsymbol{\Omega}_0$ is the direction of the solar radiation. While $I_{\mathrm{d},\nu}$ is expressed in (W m^{-2} sr^{-1} Hz^{-1}), the units of the parallel solar radiation are (W m^{-2} Hz^{-1}). In order to have a consistent set of units, the Dirac δ-function $\delta(\boldsymbol{\Omega} - \boldsymbol{\Omega}_0)$ must refer to the unit solid angle, i.e. (sr^{-1}).

According to (2.23) we may write

$$\boldsymbol{\Omega} \cdot \nabla I_\nu = \frac{dI_\nu}{ds} = \frac{dI_{\mathrm{d},\nu}}{ds} + \frac{dS_\nu}{ds}\delta(\boldsymbol{\Omega} - \boldsymbol{\Omega}_0) \tag{2.30}$$

The attenuation of the direct Sun beam S_ν along its way from the top of the atmosphere ($s = 0$) to the location s at $\mathbf{r}$ follows from *Beer's law*

$$\frac{dS_\nu}{ds} = -k_{\mathrm{ext},\nu}(s)S_\nu, \qquad \boldsymbol{\Omega} = \boldsymbol{\Omega}_0 \tag{2.31}$$